Mirrors, surfaces and maps in advanced gravitational wave detectors

Haoyu Wang

University of Shanghai for Science and Technology
Wuhan University

2021/5/7
Ando group seminar

Network of ground-based GW detectors

aLIGO, Hanford, 4km

GEO Hannover 600m

aLIGO, Livingston, 4km

AdVirgo, Cascina, 3km

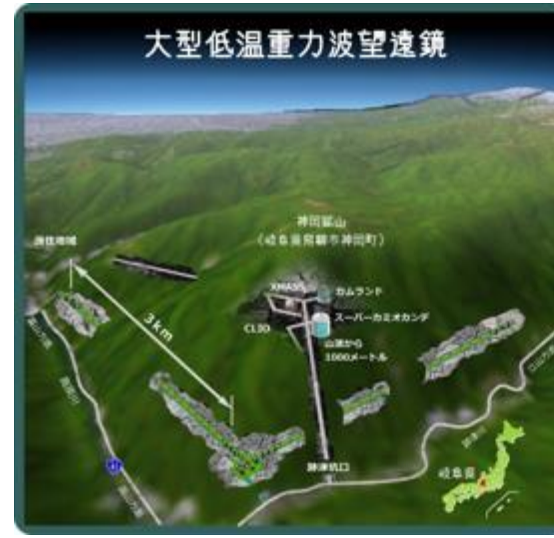

KAGRA, Kamioka, 3km

aLIGO

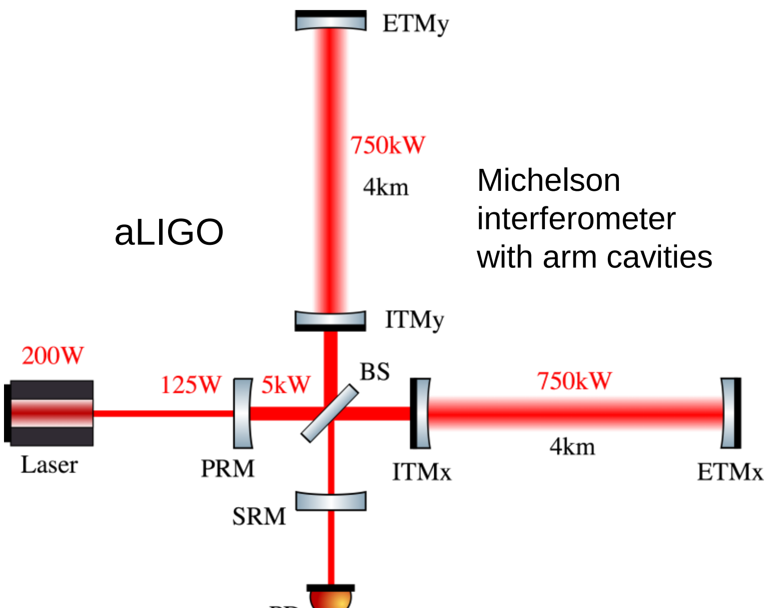

Michelson interferometer with arm cavities

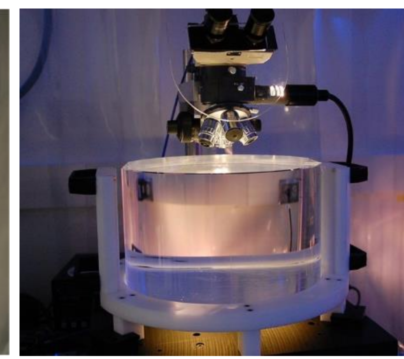

Mirrors (test masses) are critically important for GW detectors!

Key points in this talk

- Thermal modelling of test mass in Advanced LIGO
- Study the behavior of near-unstable cavities
- Simulations with mirror surface maps
- Study of the birefringence effect in KAGRA

1. Thermal modelling of aLIGO test mass

Thermal compensation system (TCS) in aLIGO

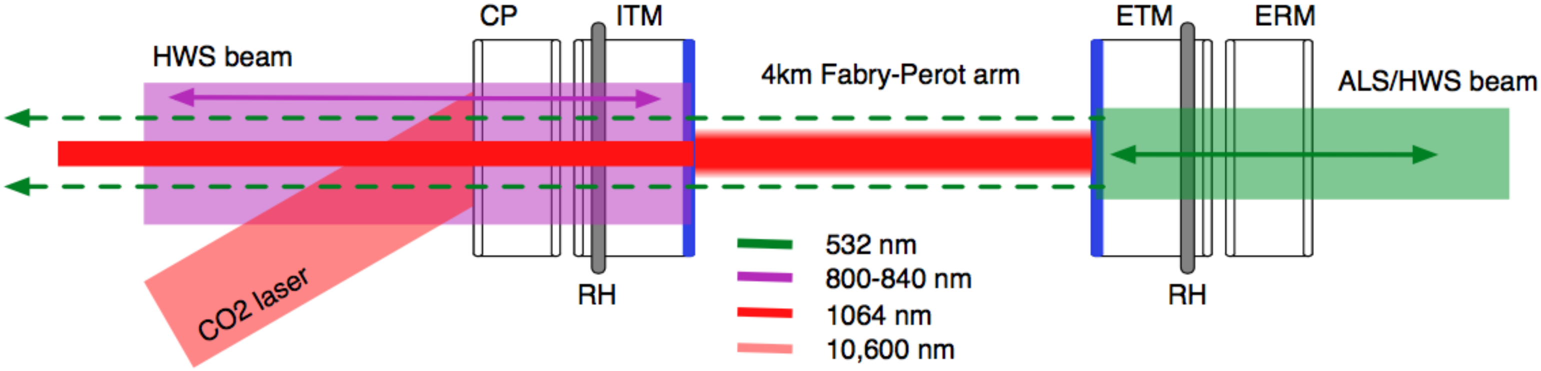

Compensation plate (CP): to compensate thermal lensing of ITM

Ring heater (RH): to compensate mirror ROC changes

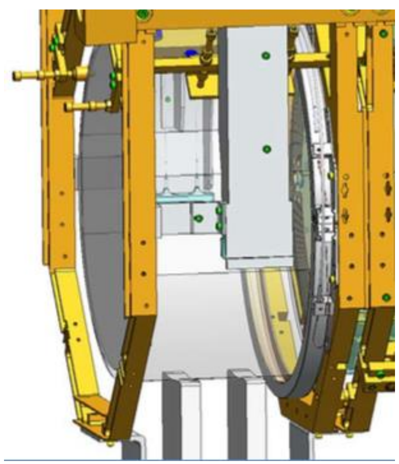

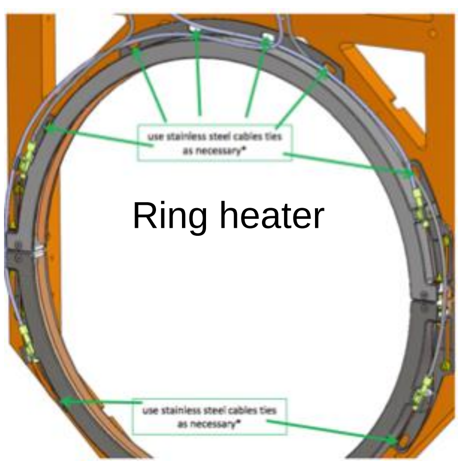

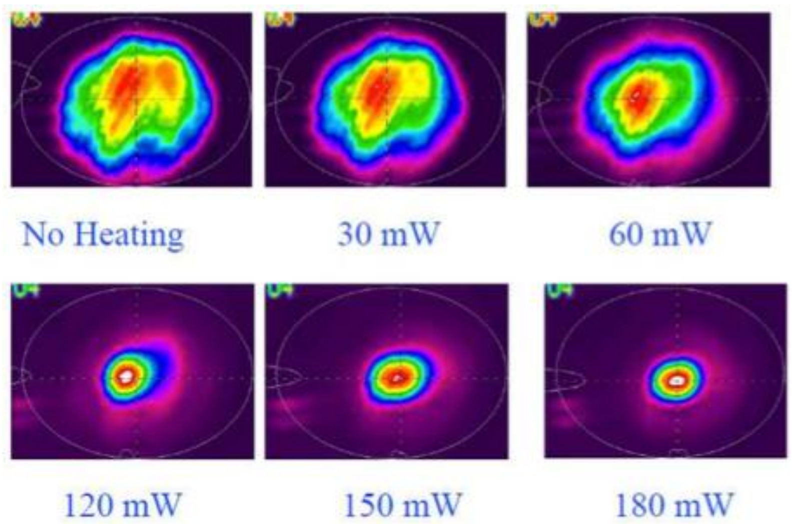

ROC accuracy: 1m around ROC of ~2000m

1. Thermal modelling of aLIGO test mass

Thermal transient impacts the performance of the high-power (750 kW) interferometer.

- Thermal lensing and expansion affects the control and sensitivity.
- Change of condition of parametric instability.

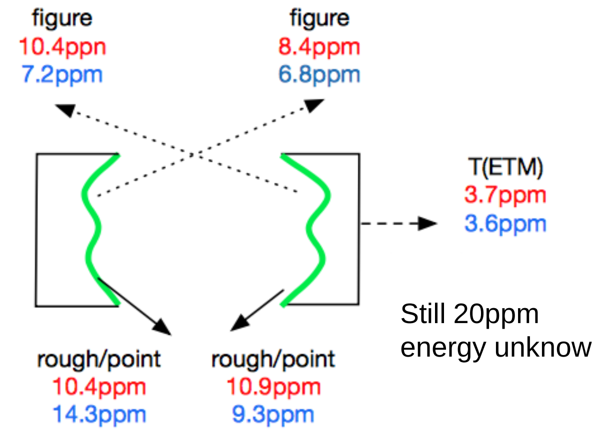

The scattered light heats surroundings near the test mass.

A good thermal model of test masses can

- help mitigate thermal effects
- give instructions for TCS for stable control
- estimate and monitor the coating absorption

The surroundings make the test mass warmer than expected.

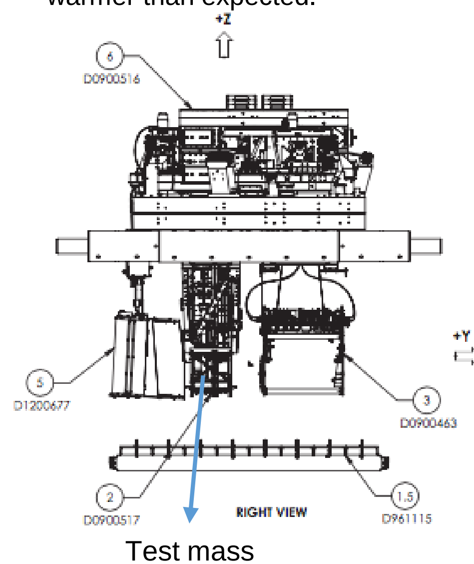

But it is not easy to accurately model thermal status of the test mass due to surroundings near the test mass.

1. Thermal modelling of aLIGO test mass

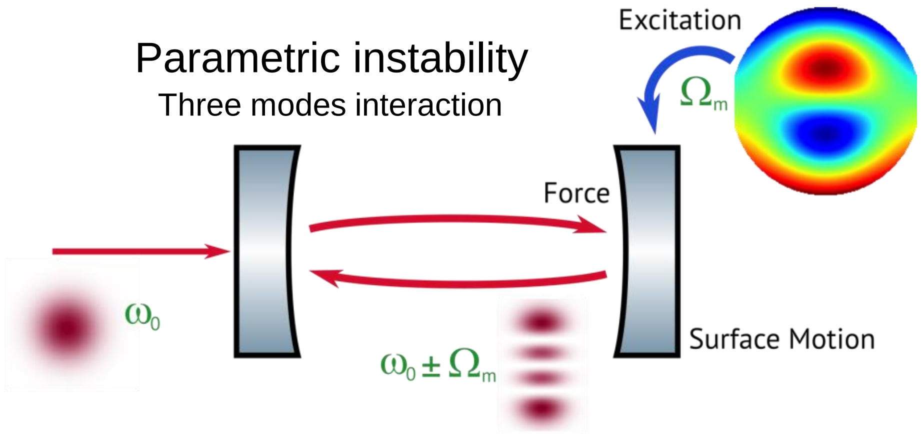

Mechanical mode frequency is used as a probe for the overall temperature of the ETM.

It is frequency is read out through the parametric instability effect.

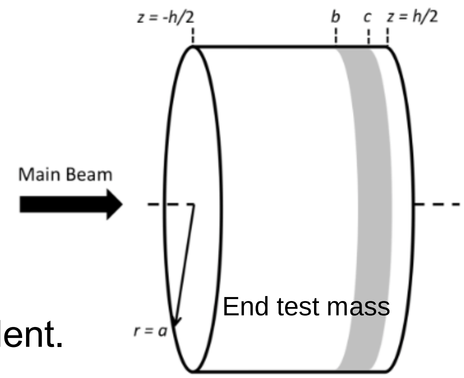

Laser 100kW → Coating absorption 1ppm (0.1W) → ΔT_{ETM} (K) → ΔE → Δf (Hz) 0.1Hz

Young's Modulus (E) is temperature dependent.

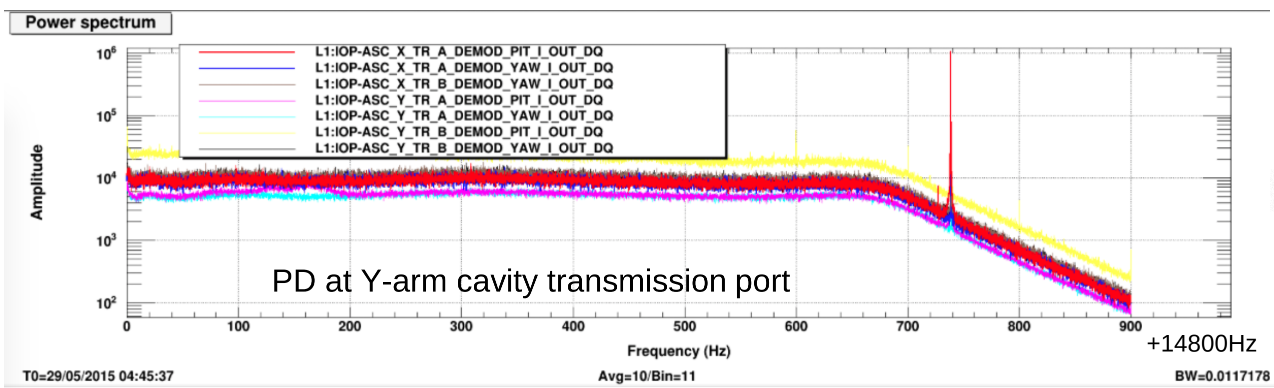

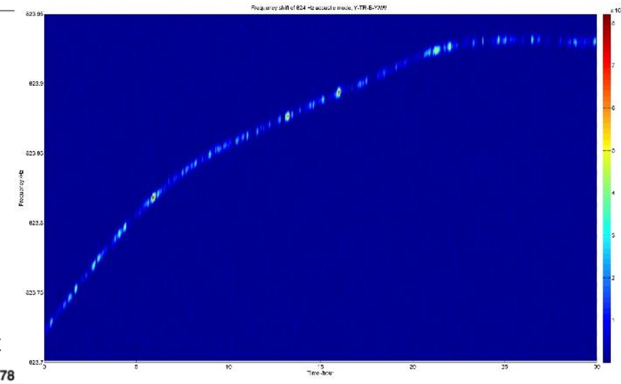

30 hours lock

1. Thermal modelling of aLIGO test mass

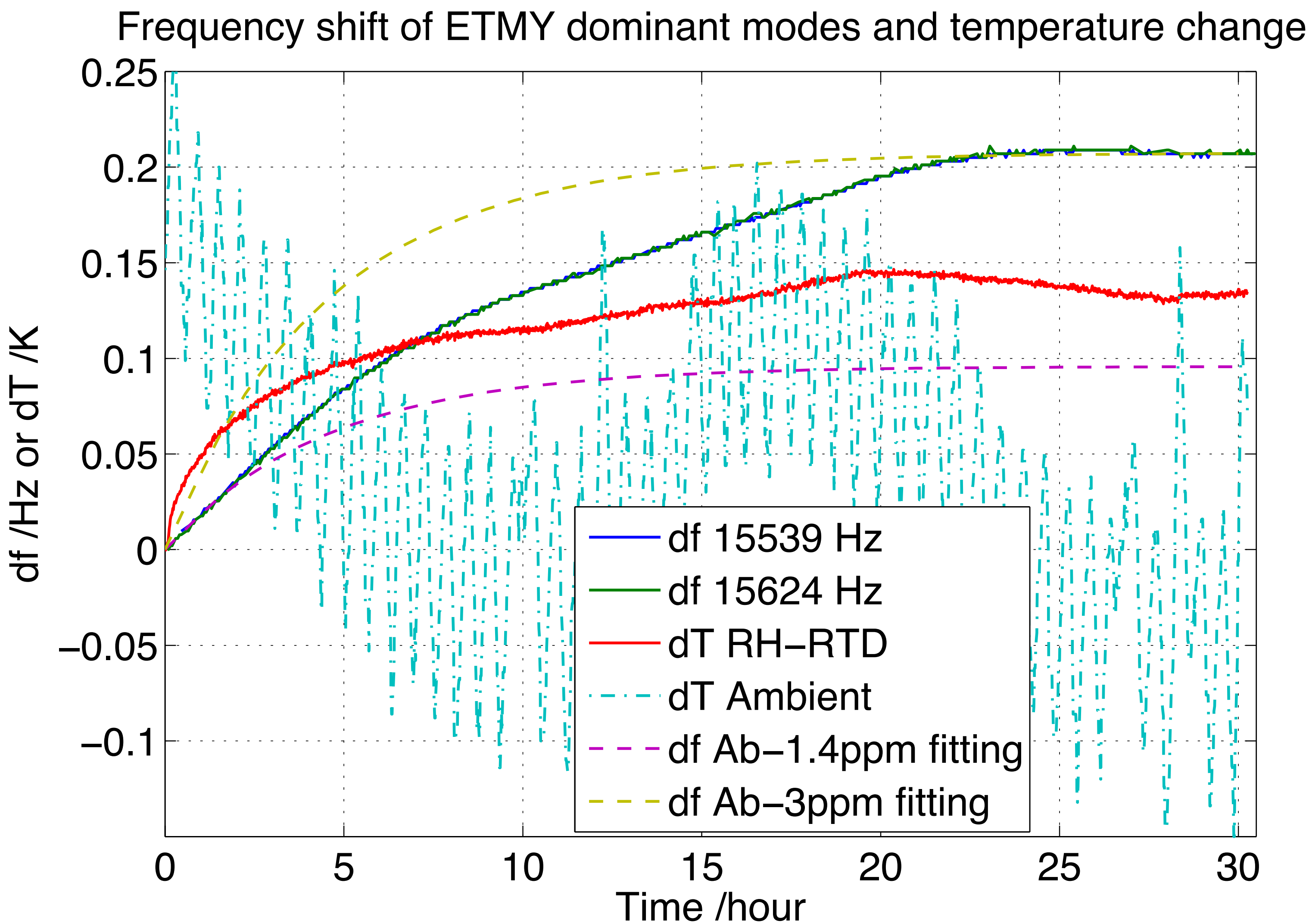

1. Thermal modelling of aLIGO test mass

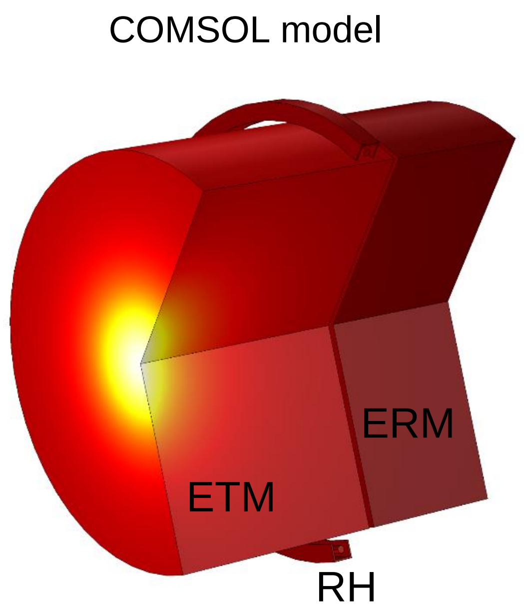

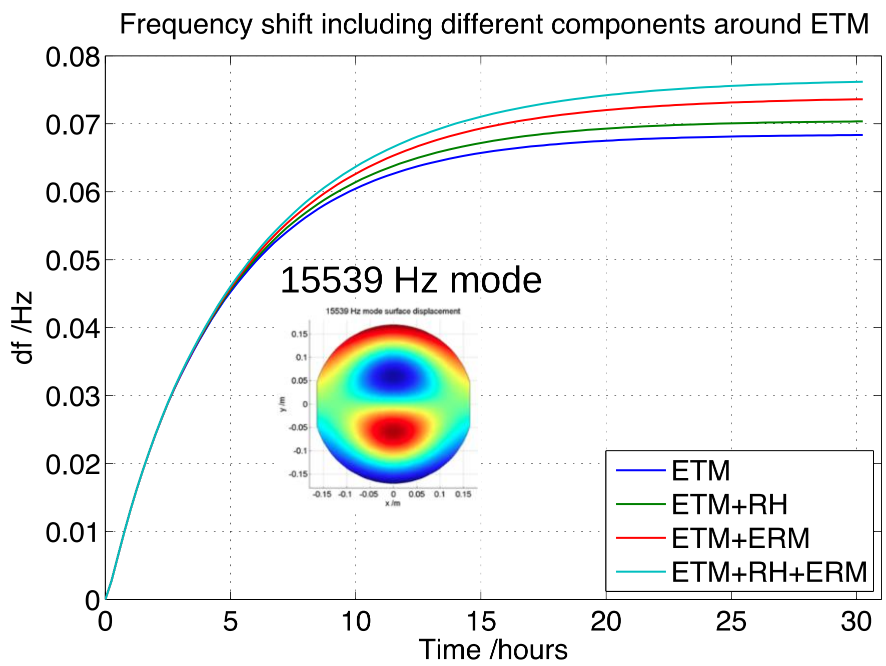

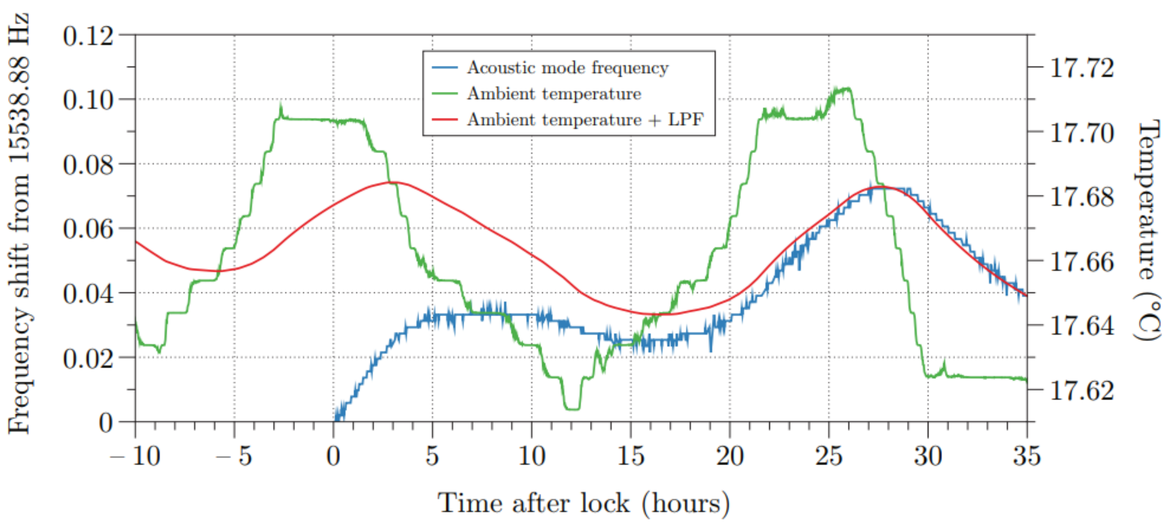

Ambient temperature calibration

A low-pass filter with a time constant of 7.2 hours is applied to the raw data.

1. Thermal modelling of aLIGO test mass

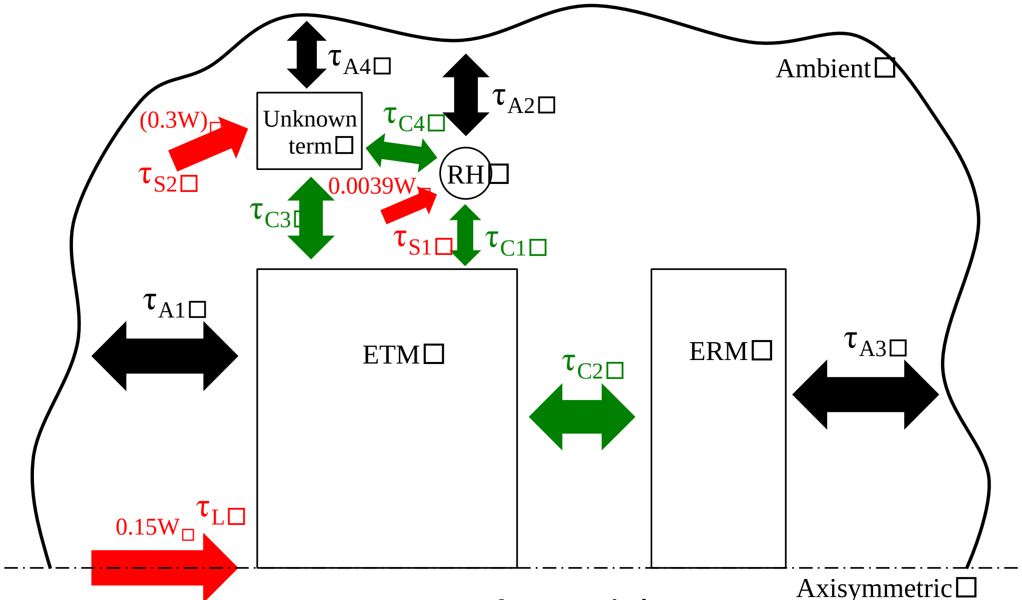

Heat transfer model

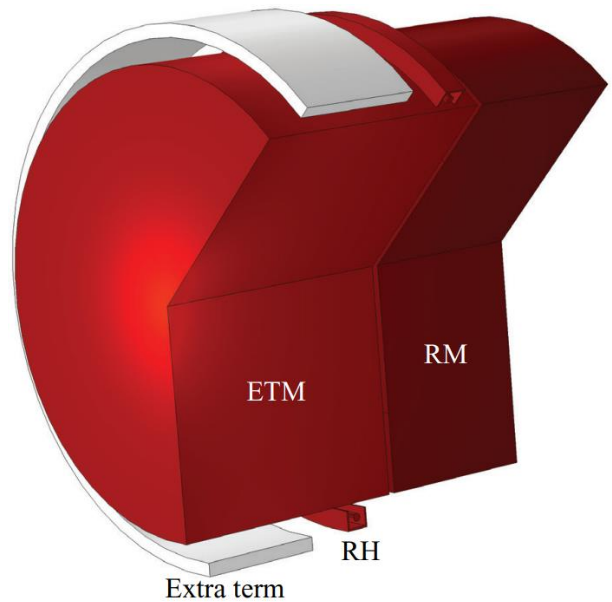

We treat each of the heat transfer mechanisms has a linear effect, as the overall temperature of the test mass by approximately 0.2°C around room temperature.

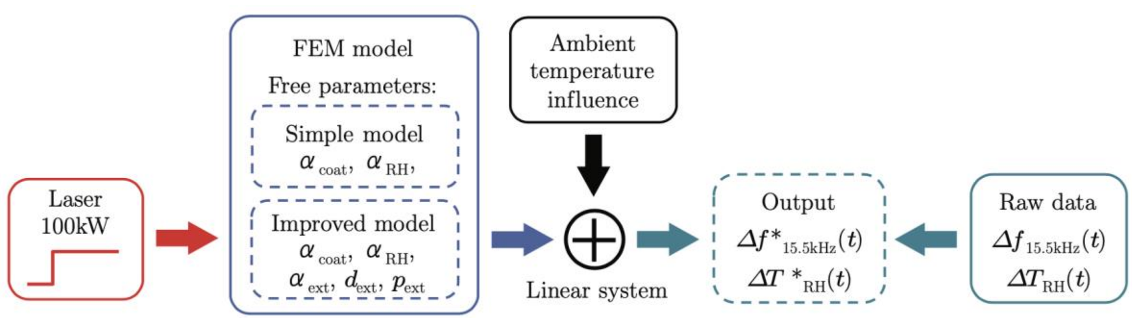

$$\Delta f_m(t) = \Delta f_{\text{laser}}(t) + \Delta f_{\text{surroundings}}(t) + \Delta f_{\text{ambient}}(t)$$

1. Thermal modelling of aLIGO test mass

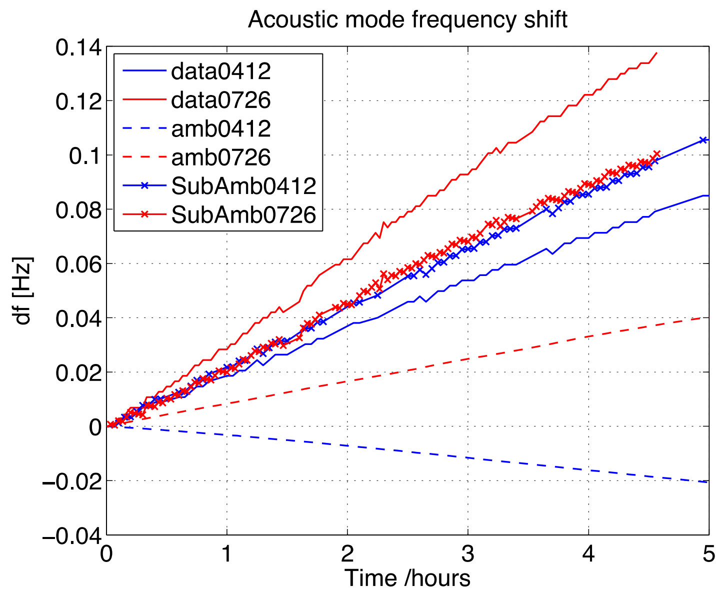

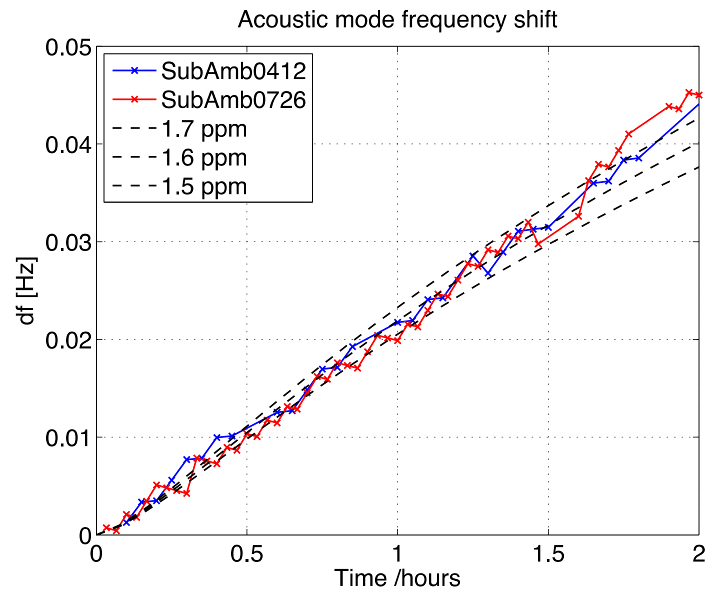

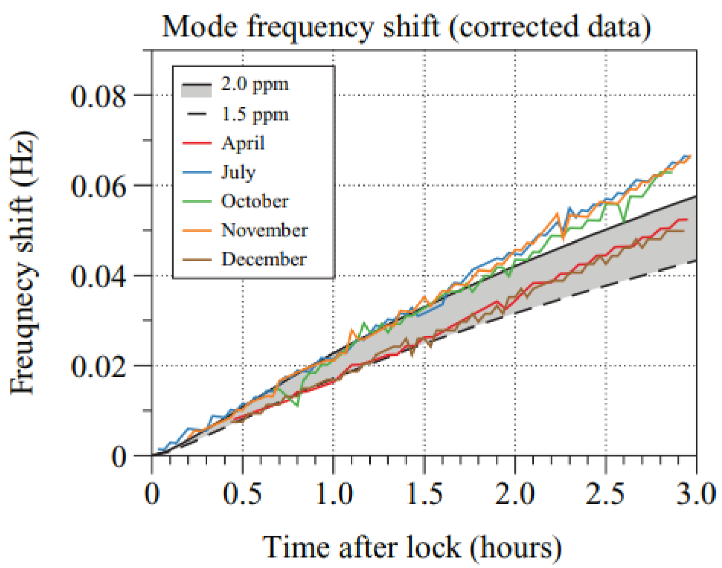

Modelling of initial hours after lock:
coating absorption: 1.5 ~ 2.0 ppm >> 0.5 ppm

1. Thermal modelling of aLIGO test mass

Long time-scale model

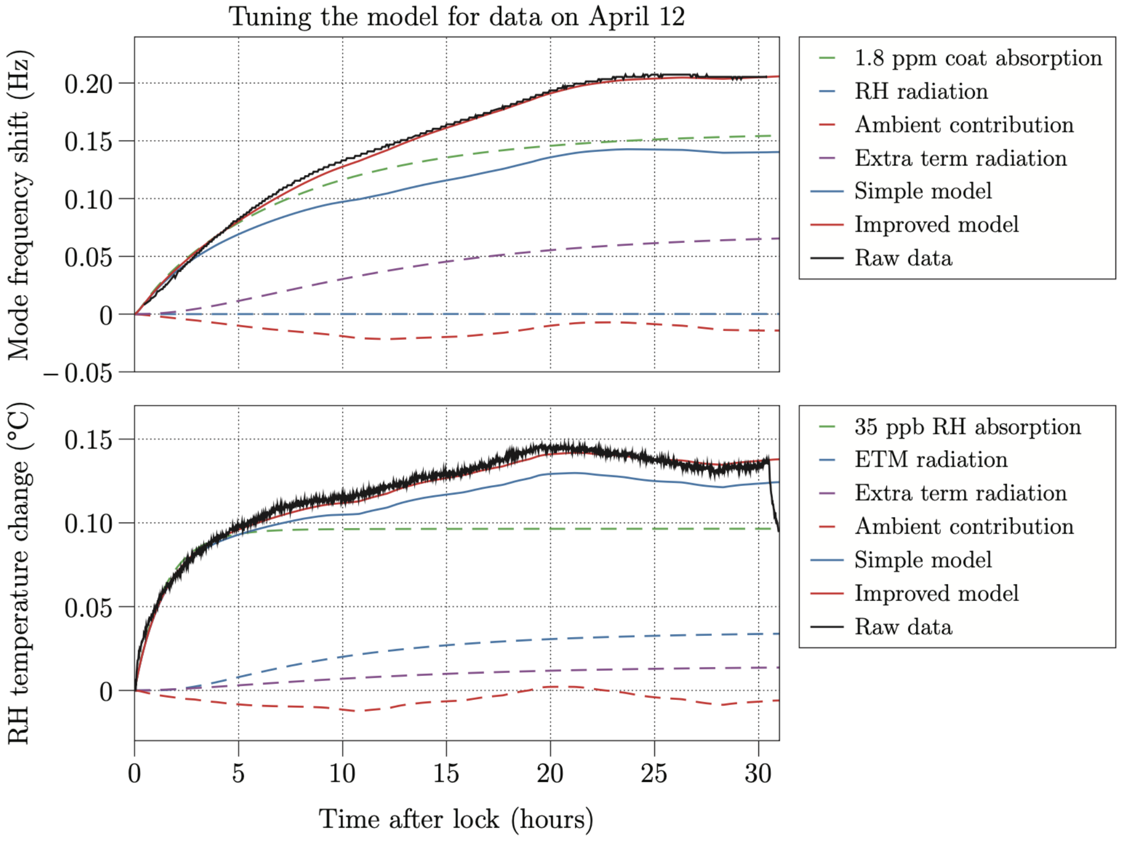

This model gives us an understand of the heating of the ETM.

We also give a model that estimates the temperature of the ring heater. The scattered light incident on the ring heater is estimated to be 0.3–1.3 ppm.

1. Thermal modelling of aLIGO test mass

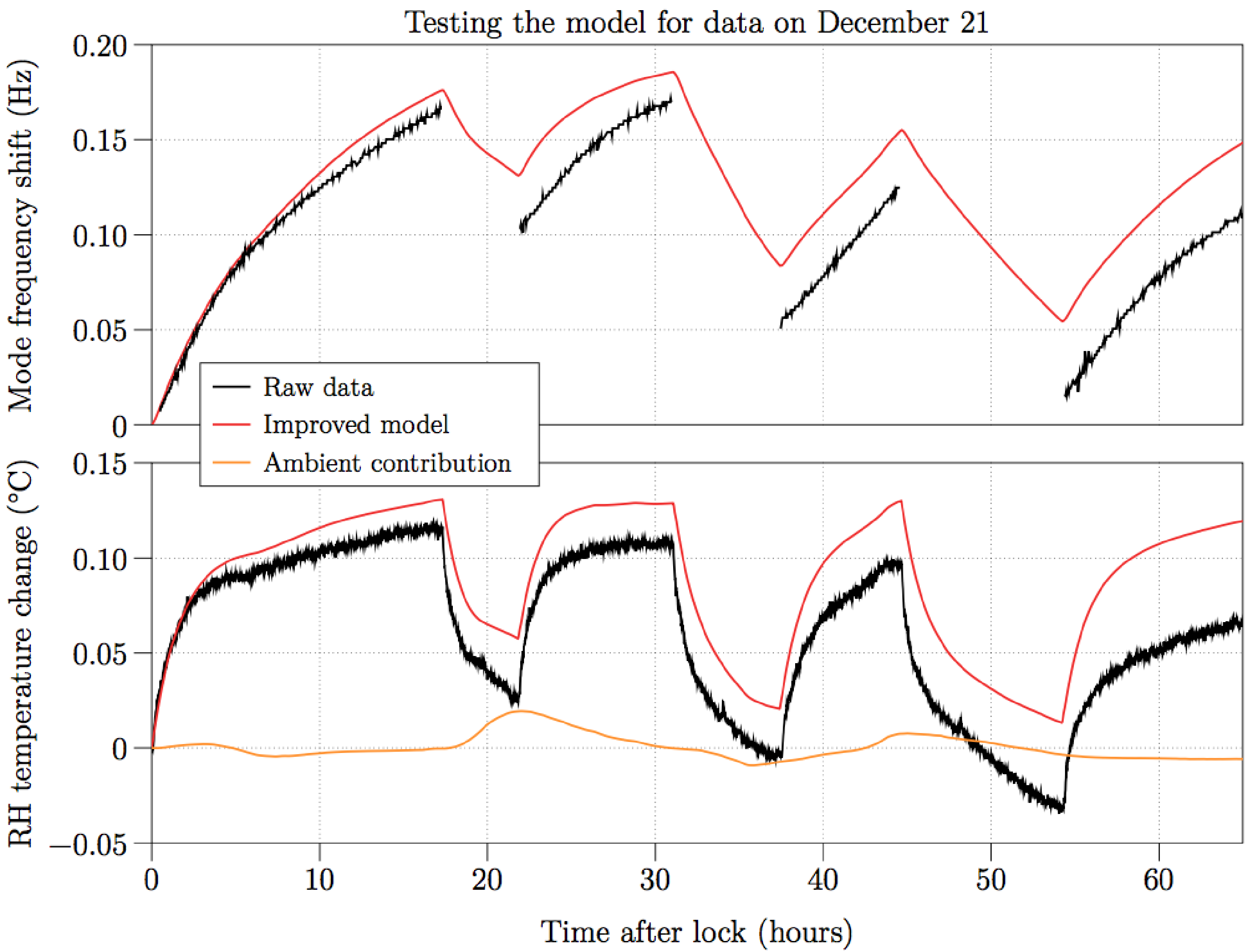

2. Study the behavior of near-unstable cavities

- From 2nd generation to 3rd generation detectors

Advanced LIGO Noise budget

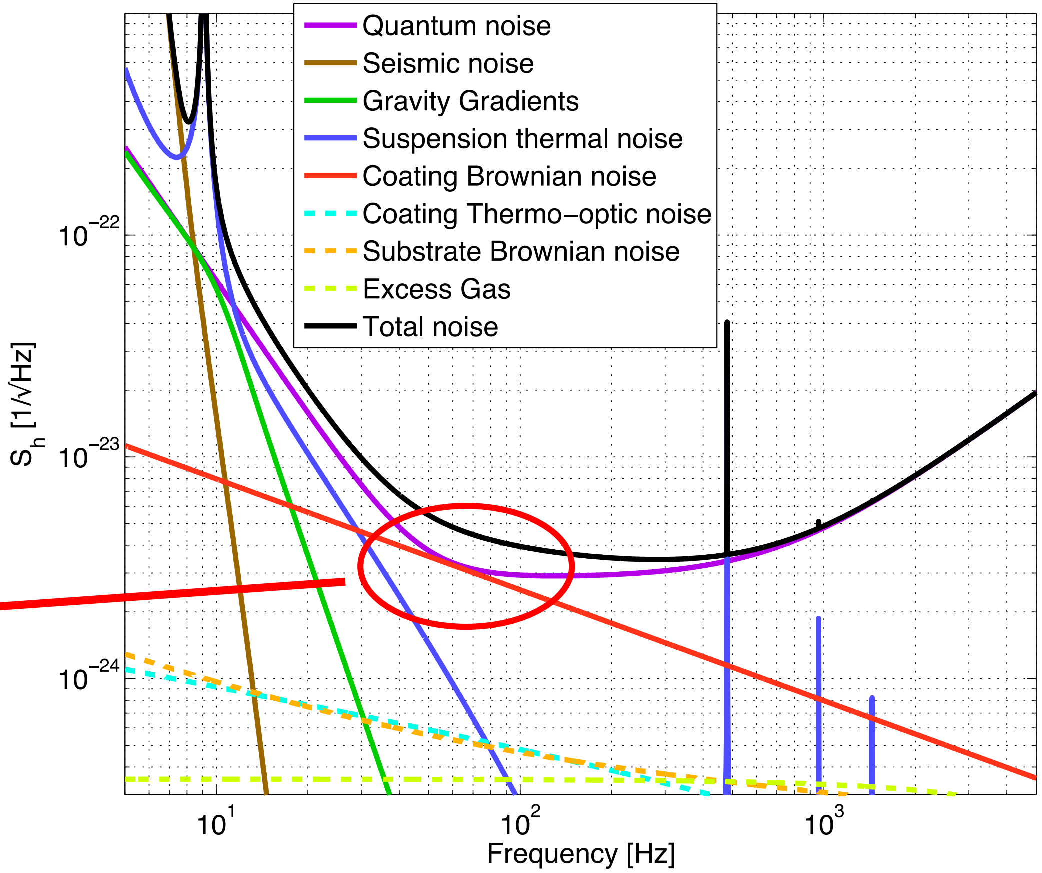

With quantum noise reduced, coating thermal noise becomes evident at mid-band.

2. Study the behavior of near-unstable cavities

- Amplitude spectral density:

temperature

coating thickness

$$S_h(f)_{coating} = \left[\frac{2k_B T}{\pi^2 L^2 f} \frac{d}{w^2 Y} \left(\frac{Y'}{Y}\phi_{\parallel} + \frac{Y}{Y'}\phi_{\perp} \right) \right]^{1/2}$$

beam spot size
on cavity mirrors

material mechanical loss

- by using cryogenic techniques: KAGRA
- by reducing coating thickness d
- by improving coatings
- by increasing beam size: averaging power on more atoms

2. Study the behavior of near-unstable cavities

- Stability criterion:

$$0 < g_1 g_2 < 1,$$

with

$$g_1 = 1 - \frac{L}{R_{c1}}$$

$$g_2 = 1 - \frac{L}{R_{c2}}$$

cavity length

radius of curvature

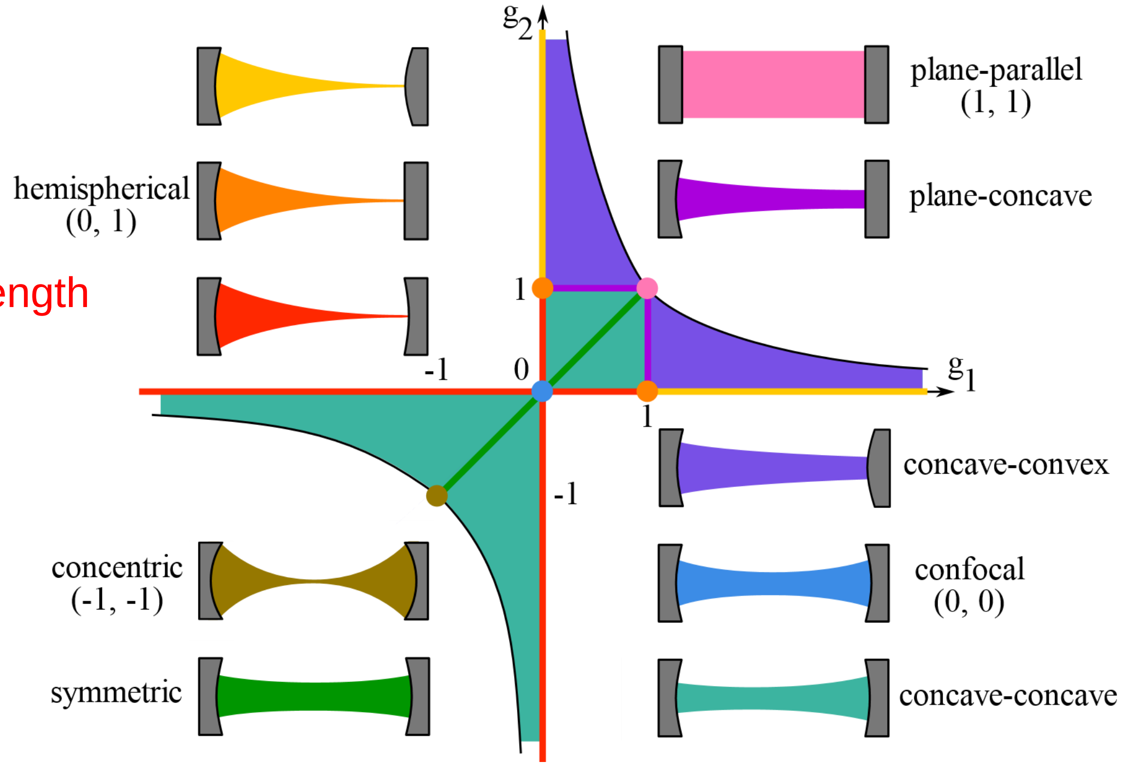

An old document: LIGO 3 Strawman Design, Team Red (LIGO DCC/public/T1200046)

Input mirror: 5.31cm -> 8.46cm (60%)

End mirror: 6.21cm -> 9.95cm (60%)

g-factor: 0.832 -> 0.974

Coating thermal noise expected to be reduced by a factor of 1.6 by using larger beam size on arm cavity mirrors

- Recycling cavities in Advanced Virgo currently are near-unstable

2. Study the behavior of near-unstable cavities

Motivation of using near-unstable cavities: large beam spots to reduce coating thermal noise

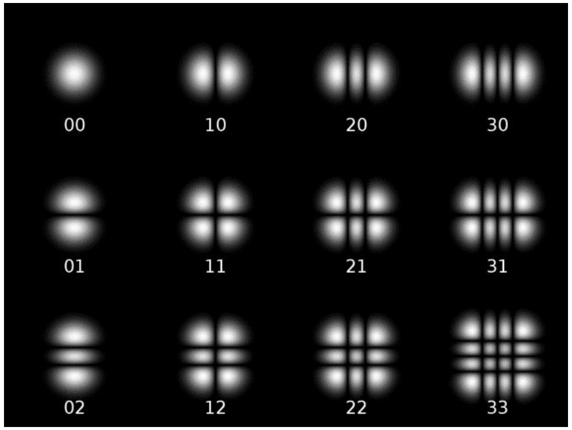

Problems:

- Mode bunching
- Easily affected by mirror defects
- Angular instability
- High optical loss
- Hard to control

One of the major difficulties of working with near-unstable cavities is that higher-order modes may become coresonant with the fundamental mode.

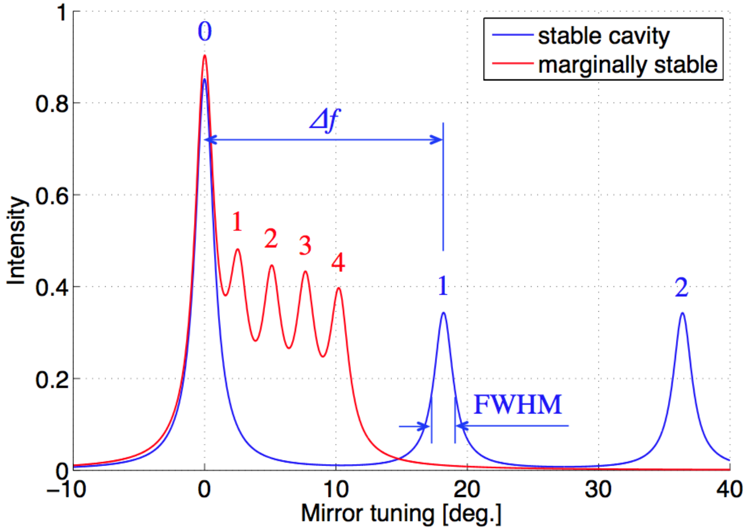

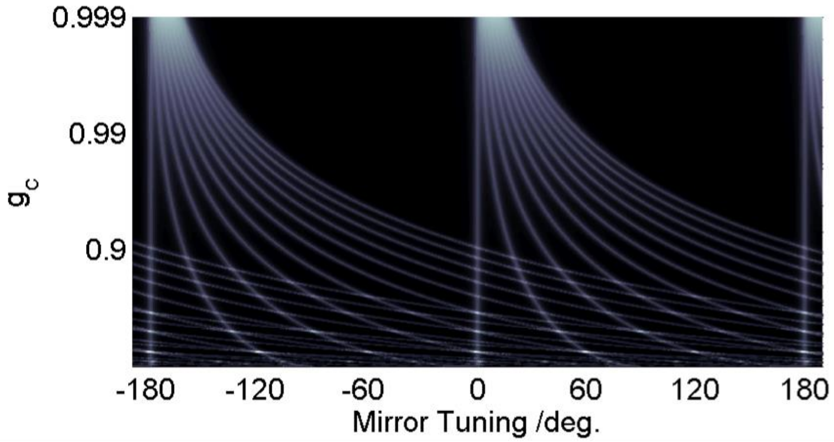

2. Study the behavior of near-unstable cavities

Goal: how far away can we go towards the stability edge without causing too much problems? https://doi.org/10.1103/PhysRevD.97.022001

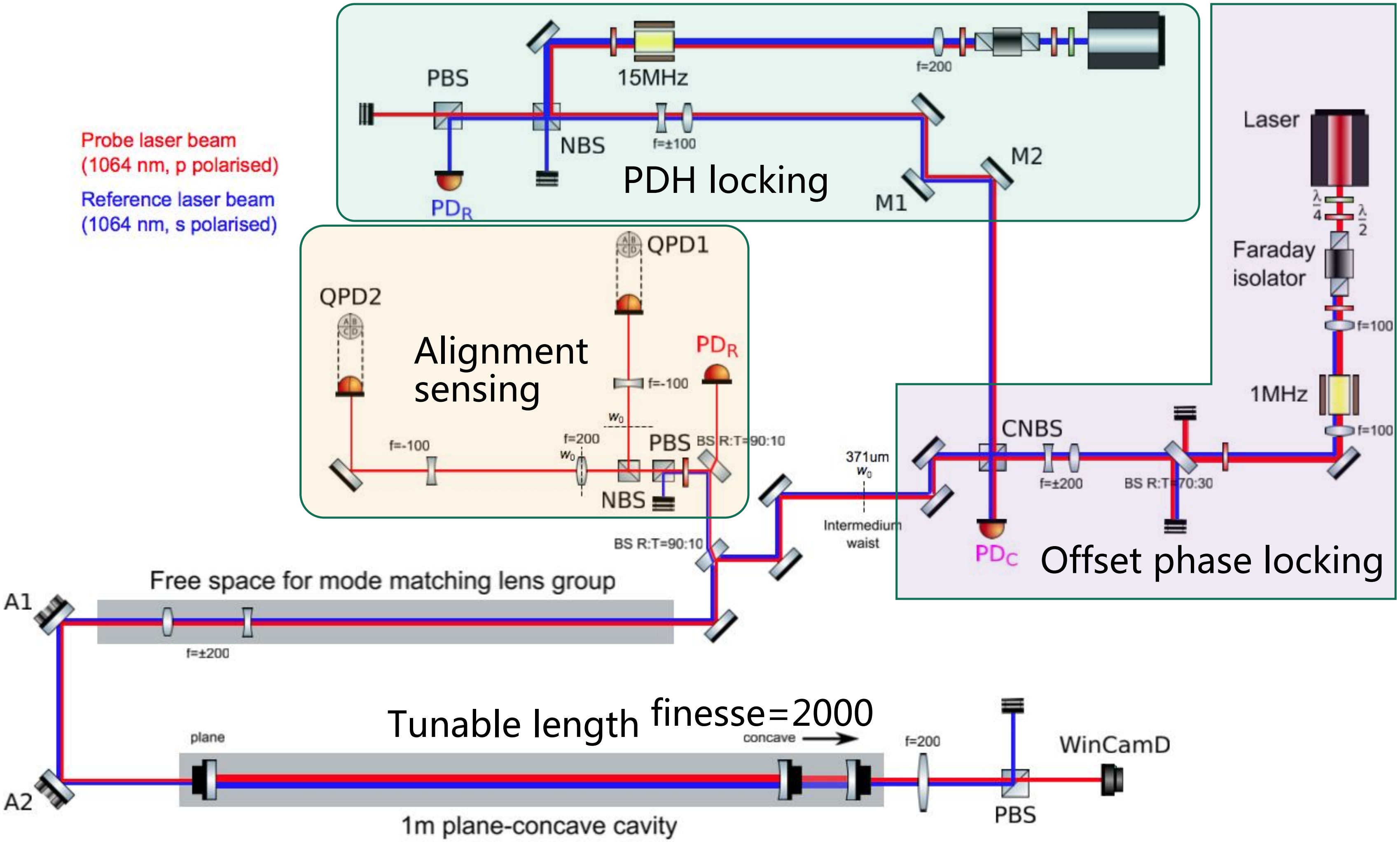

The cavity is gradually pushed to the edge of geometric stability.

2. Study the behavior of near-unstable cavities

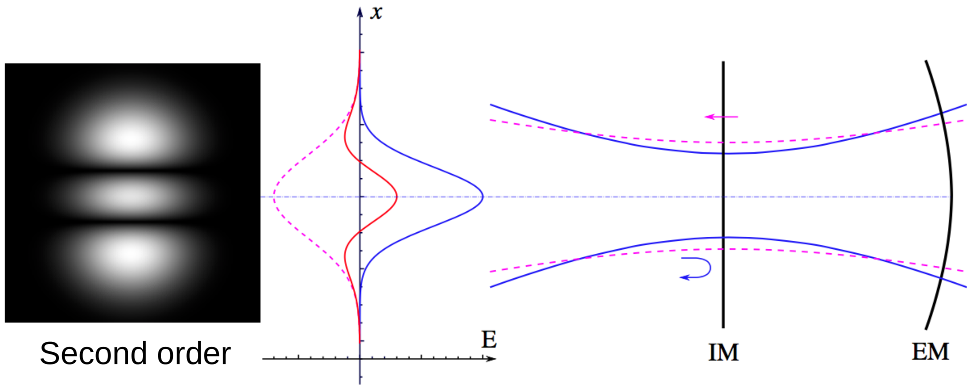

Mode mismatch

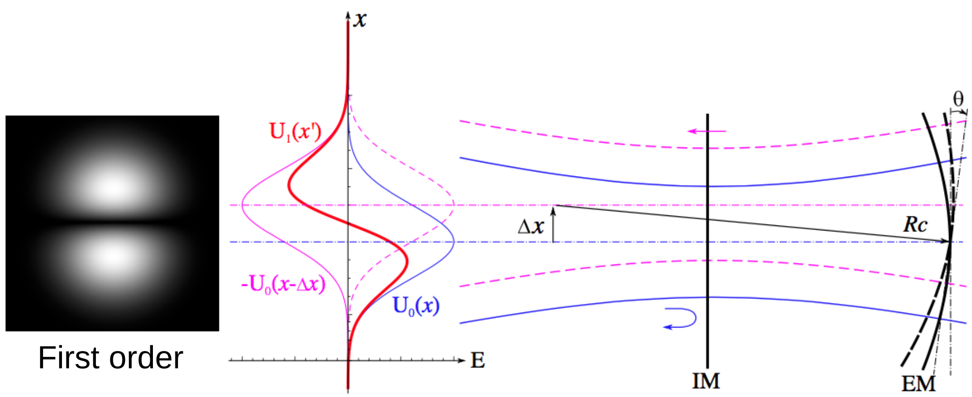

Translation

	coupling coefficient	phase
Translation Δx	$\Delta x / w_0$	$0°$
Tilt θ	$i\pi w_0 \theta / \lambda$	$90°$

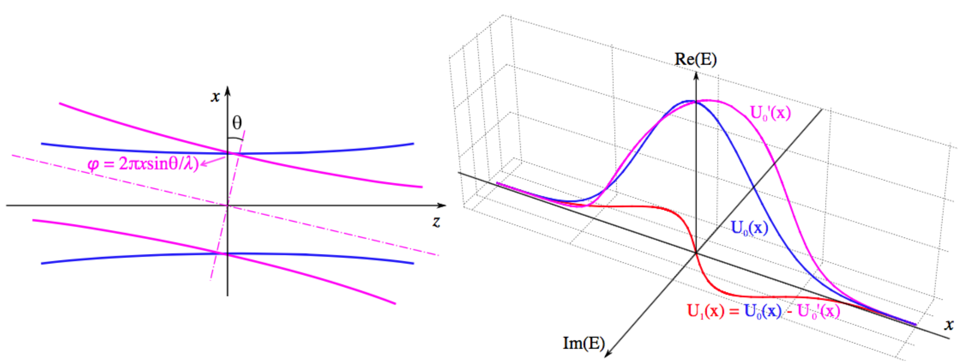

Tilt

2. Study the behavior of near-unstable cavities

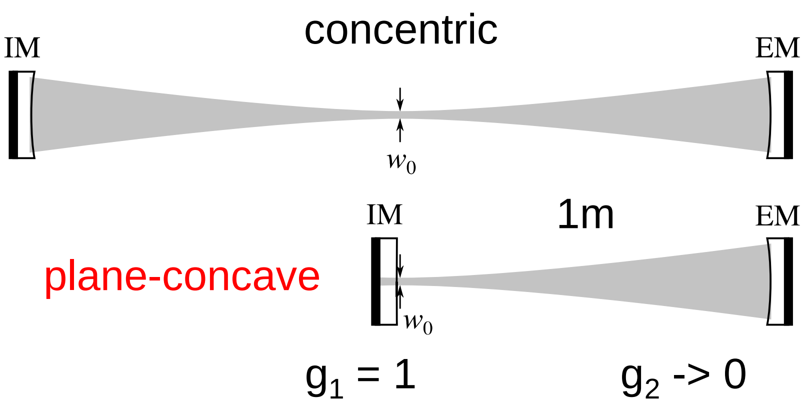

Parameters of our plane-concave cavity

Cavity length (m)	0.956	0.993	0.999	0.9999
Beam waist (μm)	263.56	168.04	103.46	58.19
Beam spot at EM (mm)	1.26	2.01	3.27	5.82
Rayleigh range (mm)	205.10	83.37	31.61	10.00
Divergent angle (mrad)	1.29	2.02	3.27	5.82
FSR (MHz)	156.80	150.95	150.05	149.91
f_1 ($\times$FSR)	0.433	0.474	0.490	0.497
f_2 ($\times$FSR)	0.865	0.947	0.980	0.994
δ_2	563.2	223.2	84.6	26.6
g_c	0.044	0.007	0.001	0.0001
g_c^*	0.832	0.972	0.996	0.9996

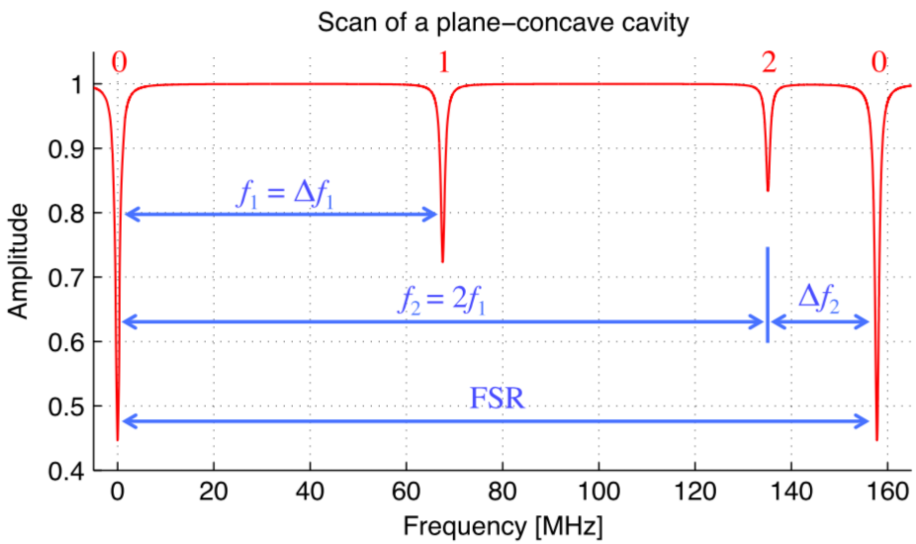

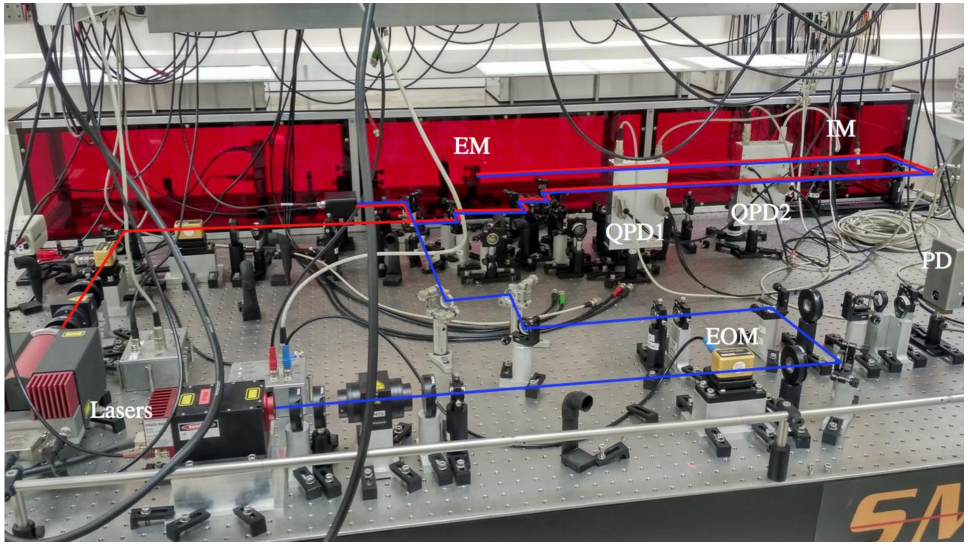

2. Experiments on near-unstable cavities

Mode splitting observed

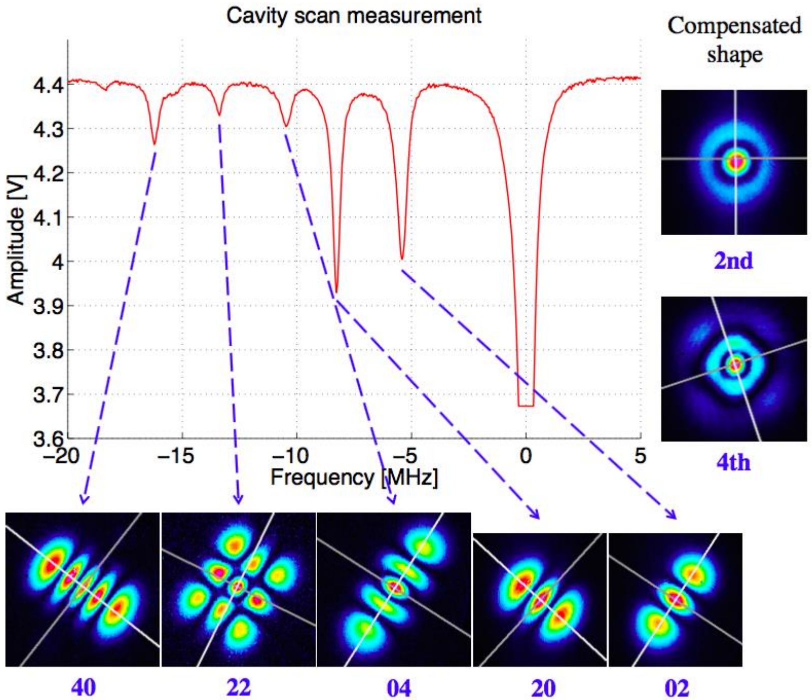

Mode splitting observed (measurement)

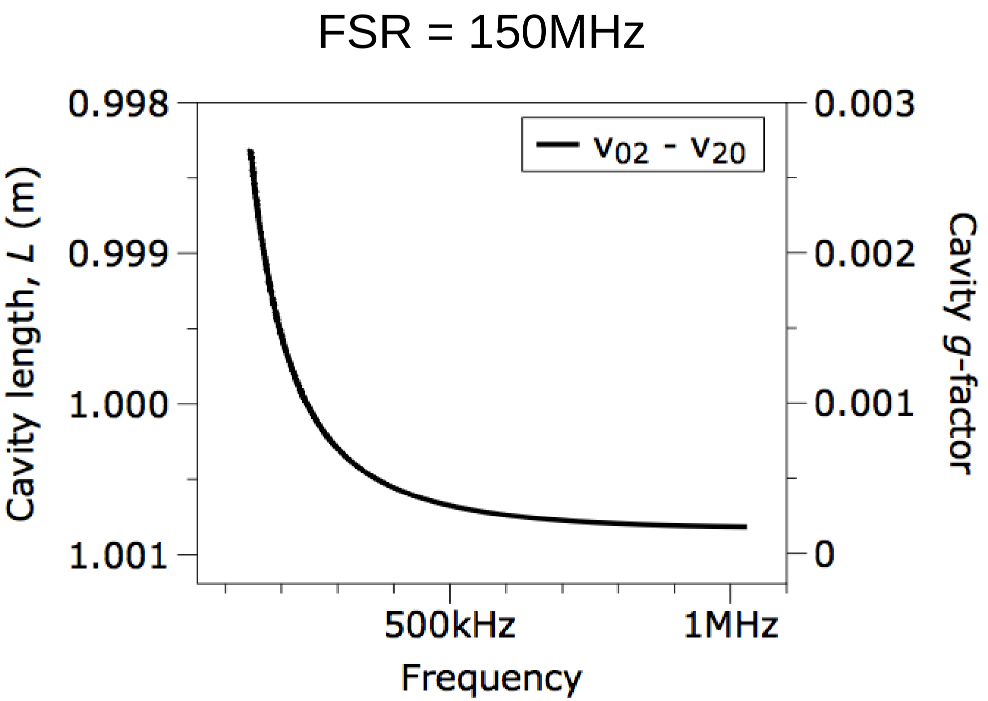

Mode splitting as a function of g-factor (simulation)

The surface of the EM is ellipsoidal.

The separation can be reduced by increasing the stress of the screw holding the spherical mirror, thus compensating the surface deformation.

2. Experiments on near-unstable cavities

We measure resonant frequencies of 2nd modes and the fundamental mode.

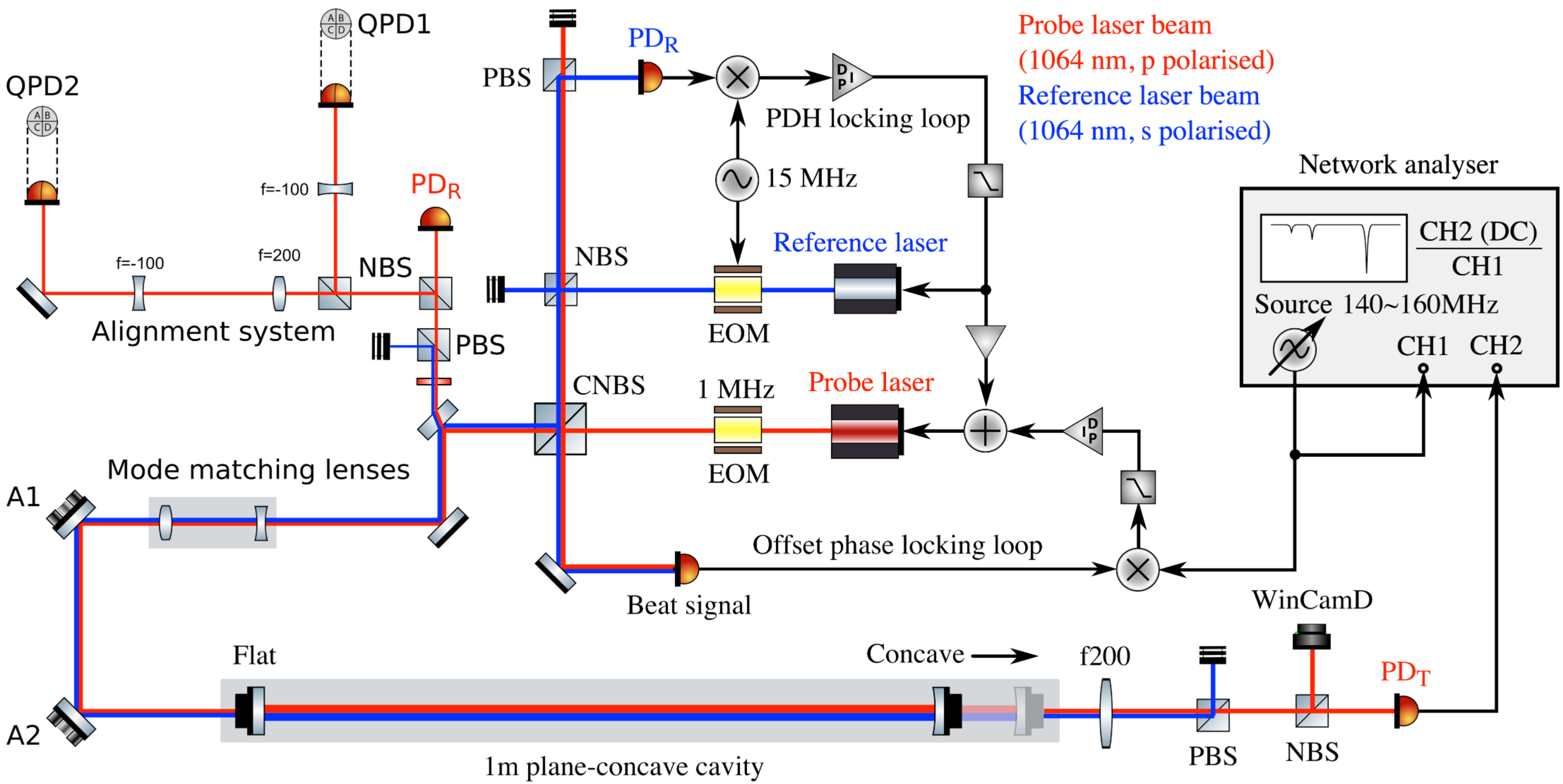

2. Experiments on near-unstable cavities

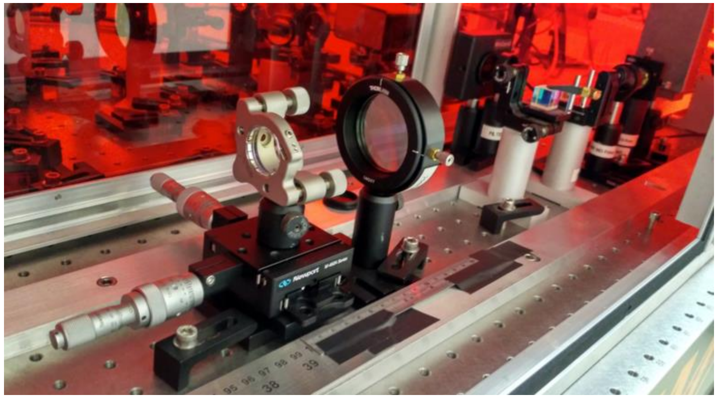

Cavity length as a function of mode spacing frequency for the plane-concave cavity

$$L_0 + \Delta L = \frac{R_c}{2}\left[1 - \cos\left(\frac{\Delta f^{02}}{\mathrm{FSR}}\pi\right)\right]$$

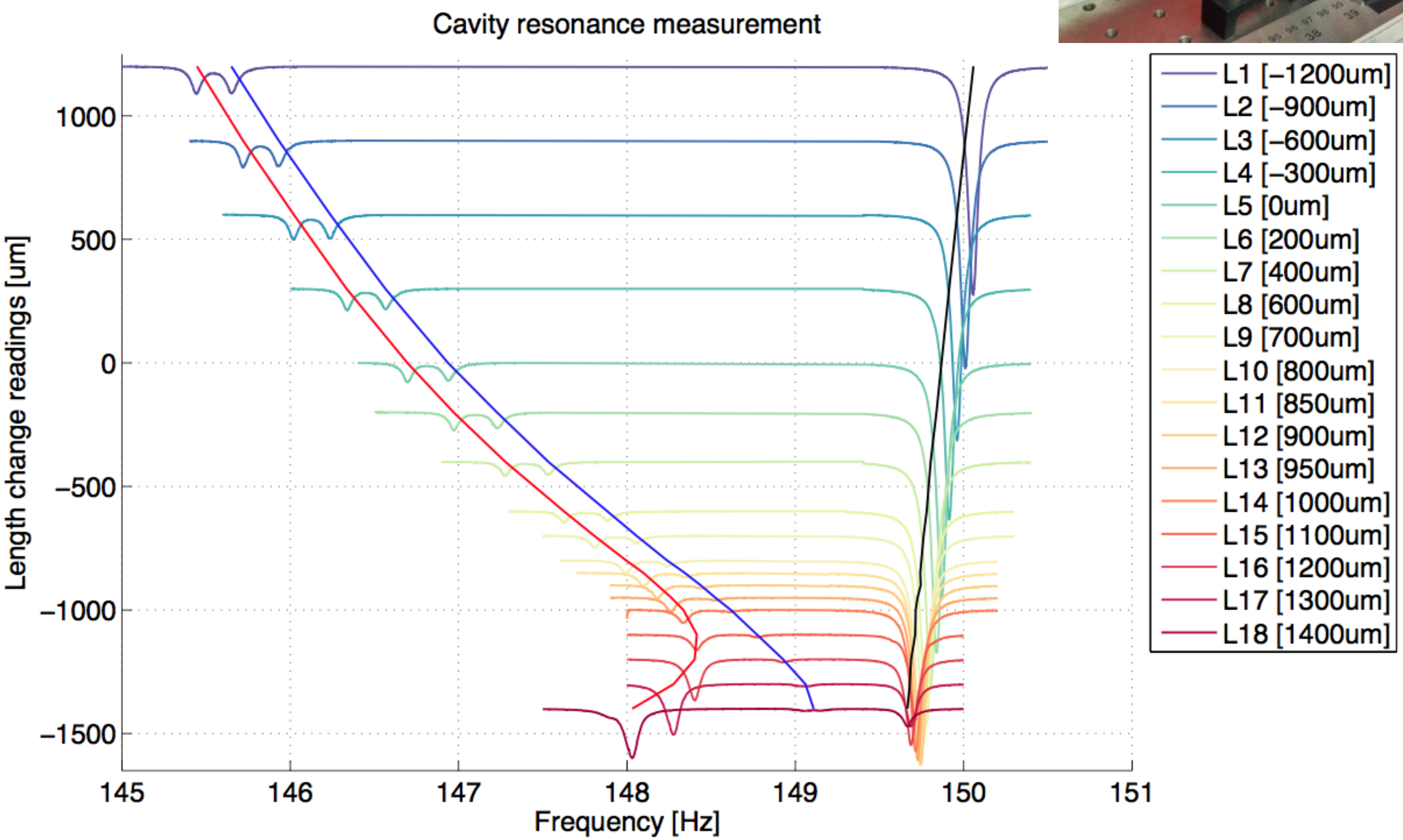

We change the position of the concave end mirror via a translation stage and take 18 measurements.

The mode matching is very difficult.

sum of HG00 and HG20 modes

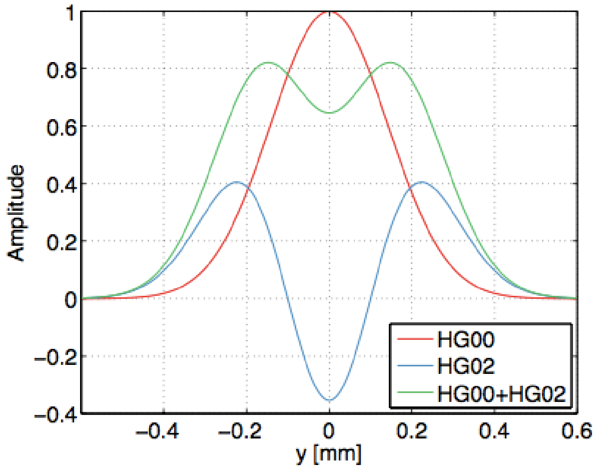

Measured modes' frequencies

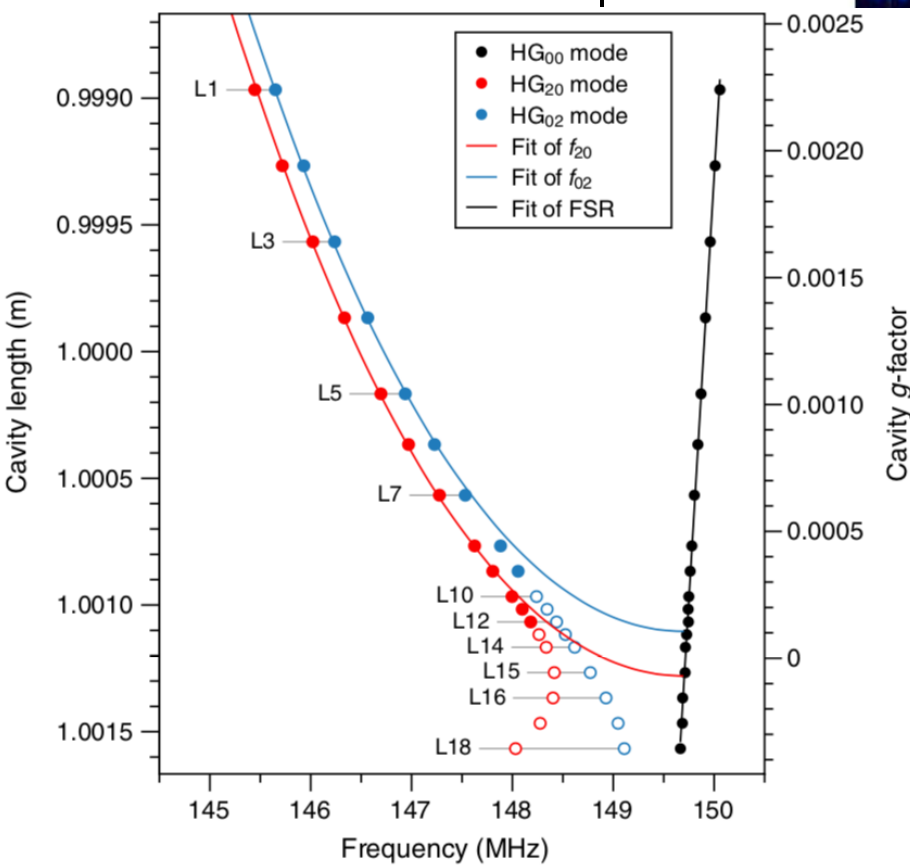

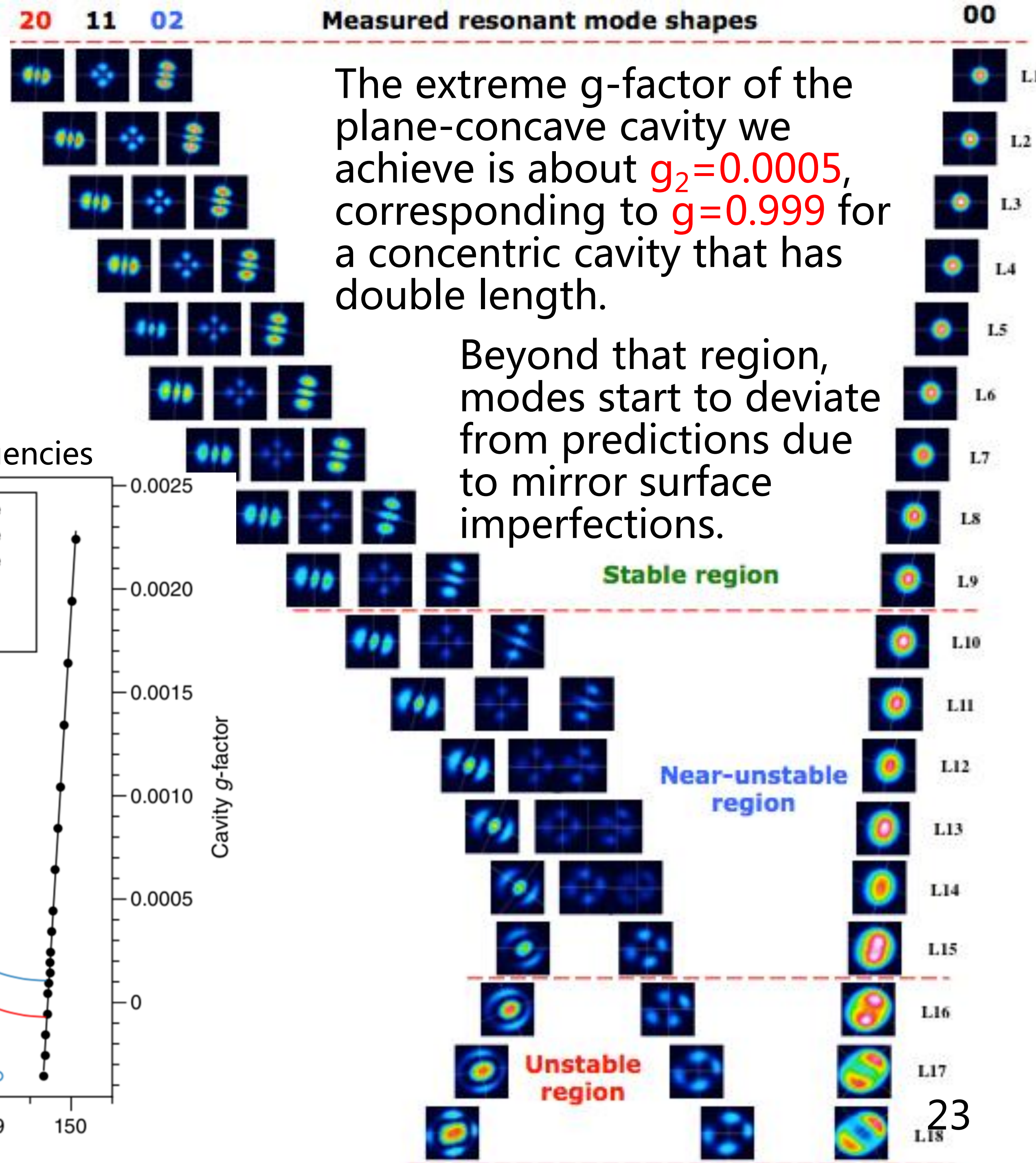

The extreme g-factor of the plane-concave cavity we achieve is about g_2=0.0005, corresponding to g=0.999 for a concentric cavity that has double length.

Beyond that region, modes start to deviate from predictions due to mirror surface imperfections.

3. Simulation with mirror maps

The measured mirror map can be applied the the EM in FINESSE.

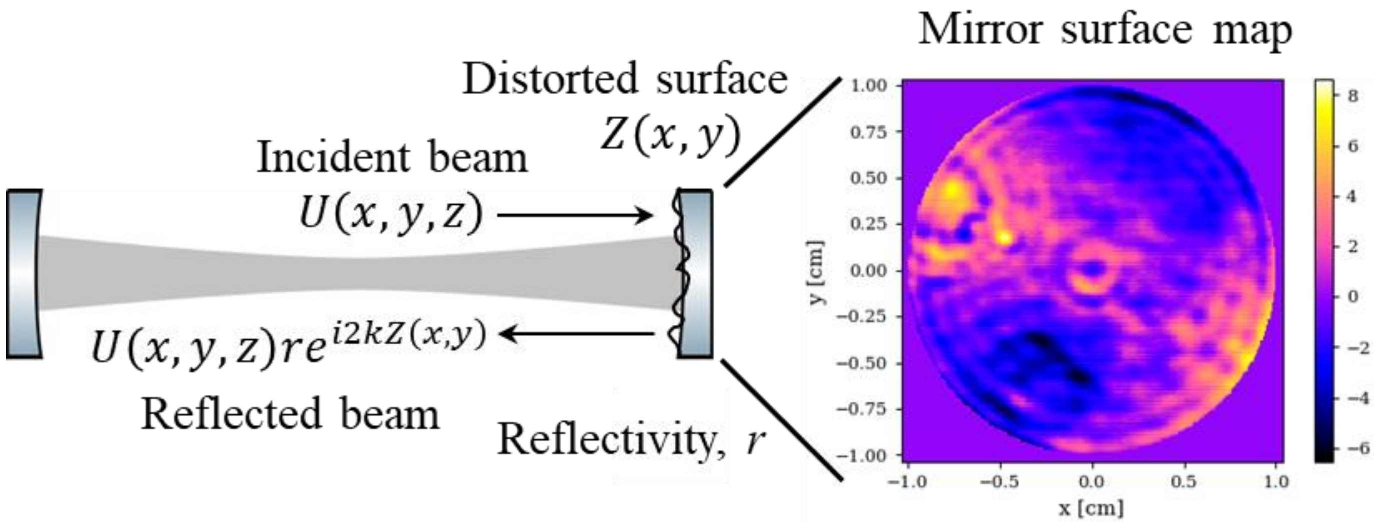

Coupling coefficients for TEM mode

$$k_{n,m,n',m'} = \exp\left(\mathrm{i}\,2kz'\sin^2\left(\frac{\gamma}{2}\right)\right)\iint dx'dy'\ u_{n'm'}\exp\left(\mathrm{i}\,kx'\sin\gamma\right)\ u^*_{nm}$$

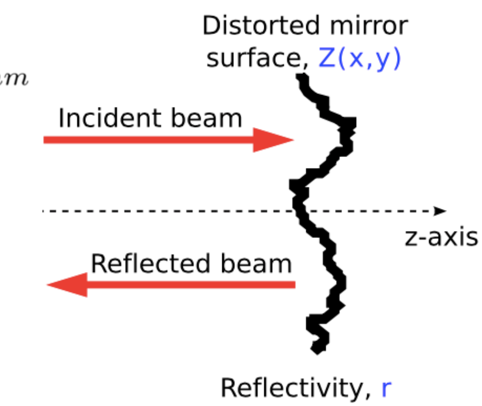

Goal:

- Trying to understand mode behaviors.
- Trying to model mirror defect influences.

3. Simulation with mirror maps

Finesse is a widely-used interferometer simulation program in GW community.

Finesse 2

Andreas Freise

A number of desired analysis for modelling modern complex gravitational wave interferometers can be performed, like computing

- modulation-demodulation error signals
- transfer functions
- control matrix
- quantum-noise-limited sensitivities
- scattering effects
- beam shapes

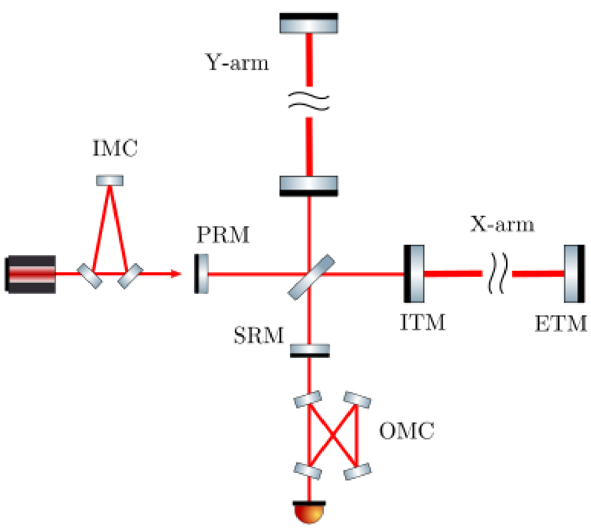

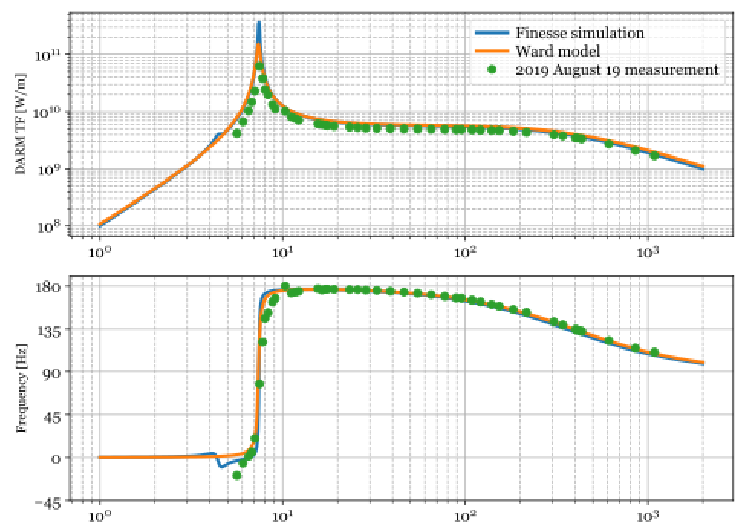

Fitting the frequency change

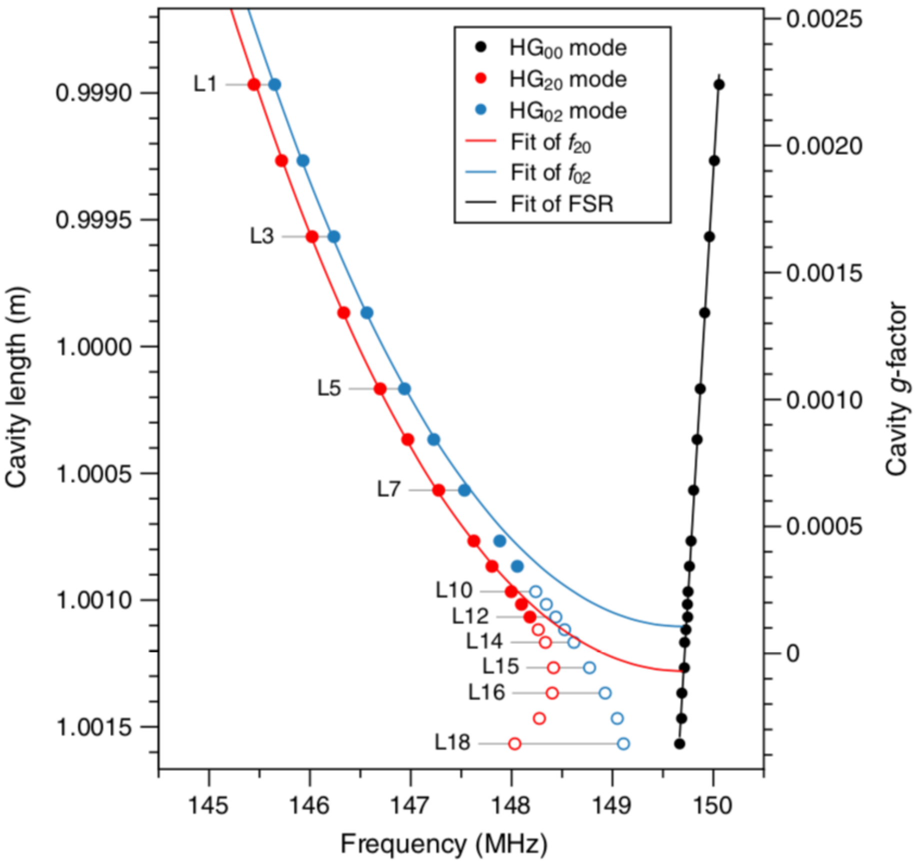

$$L_0 + \Delta L = \frac{R_{2+}}{2}\left[1 - \cos\left(\frac{f_{20}}{\mathrm{FSR}}\pi\right)\right]$$

$$L_0 + \Delta L = \frac{R_{2-}}{2}\left[1 - \cos\left(\frac{f_{02}}{\mathrm{FSR}}\pi\right)\right]$$

R_{2+} = 1,001,284.9 ± 4.6 μm
R_{2-} = 1,001,140.0 ± 15.7 μm
The difference is about 145 μm

ZYGO measurement

The mirror map: phase map

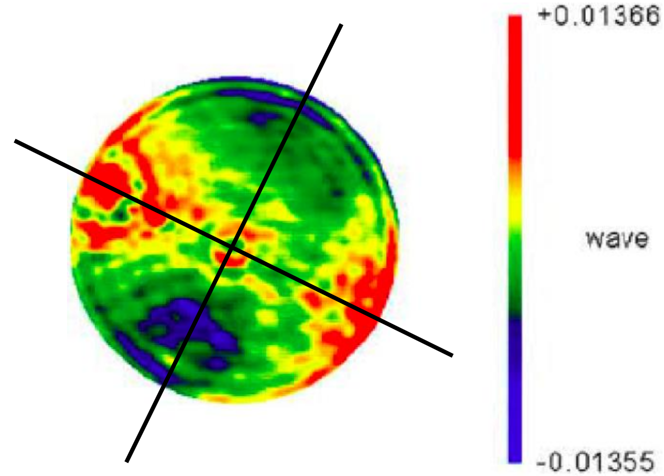

PV: 17.2nm RMS: 2.2nm

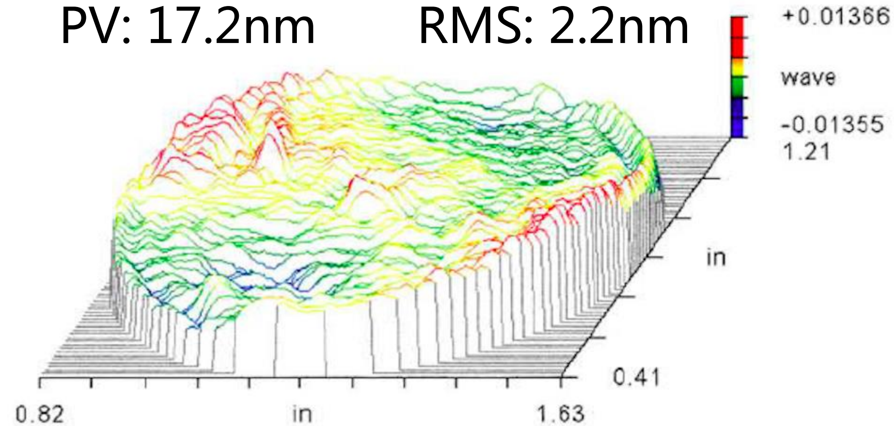

By fitting mode frequency changes,

- we can quantify the stability
- study mode behaviors
- it is possible to infer the shape of the mirror surface

3. Simulation with mirror maps

Fitting the map with Zernike polynomials

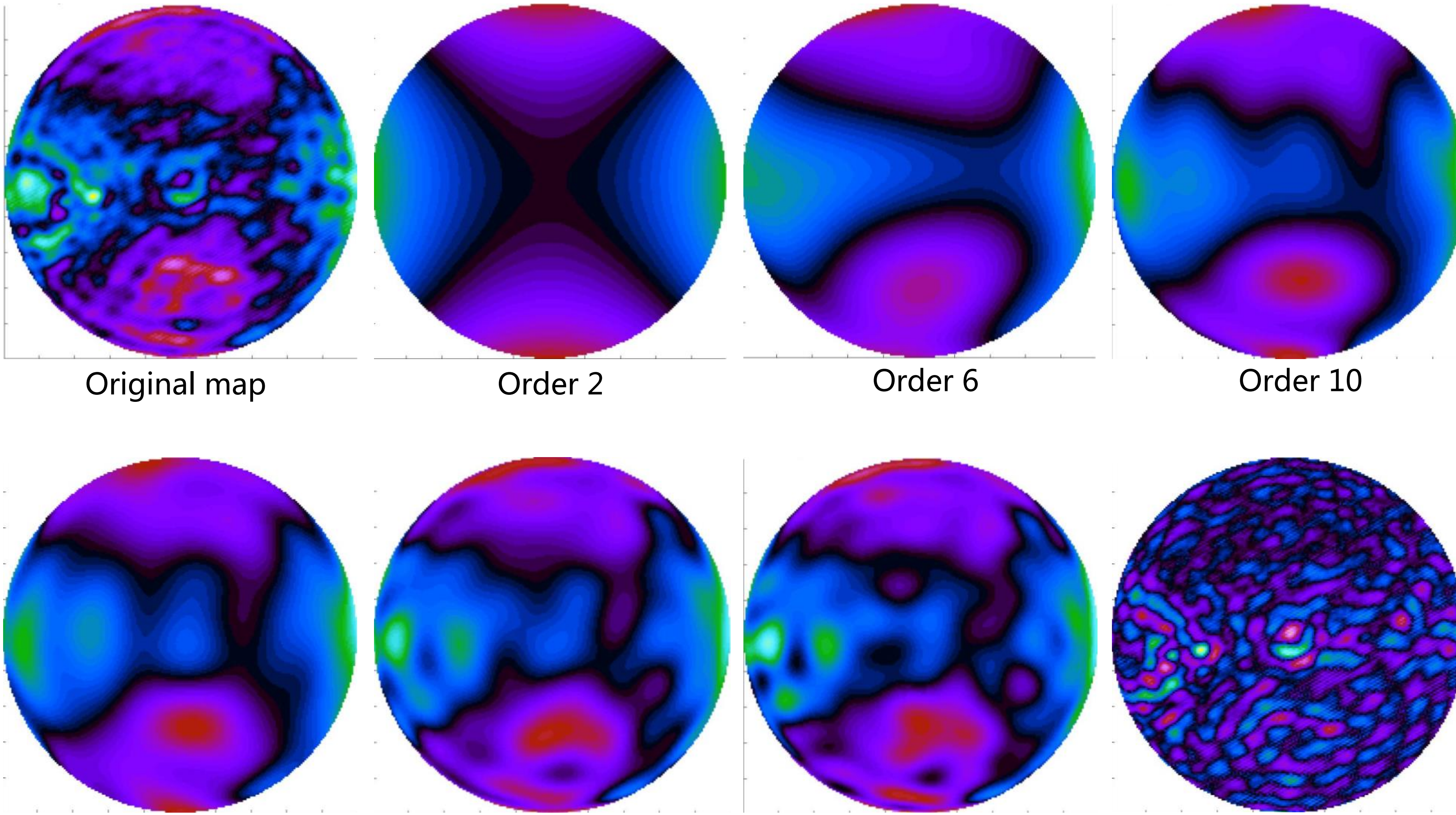

Original map
Order 2
Order 6
Order 10
Order 12
Order 16
Order 20
Residue of order 20

Fitting the frequency change

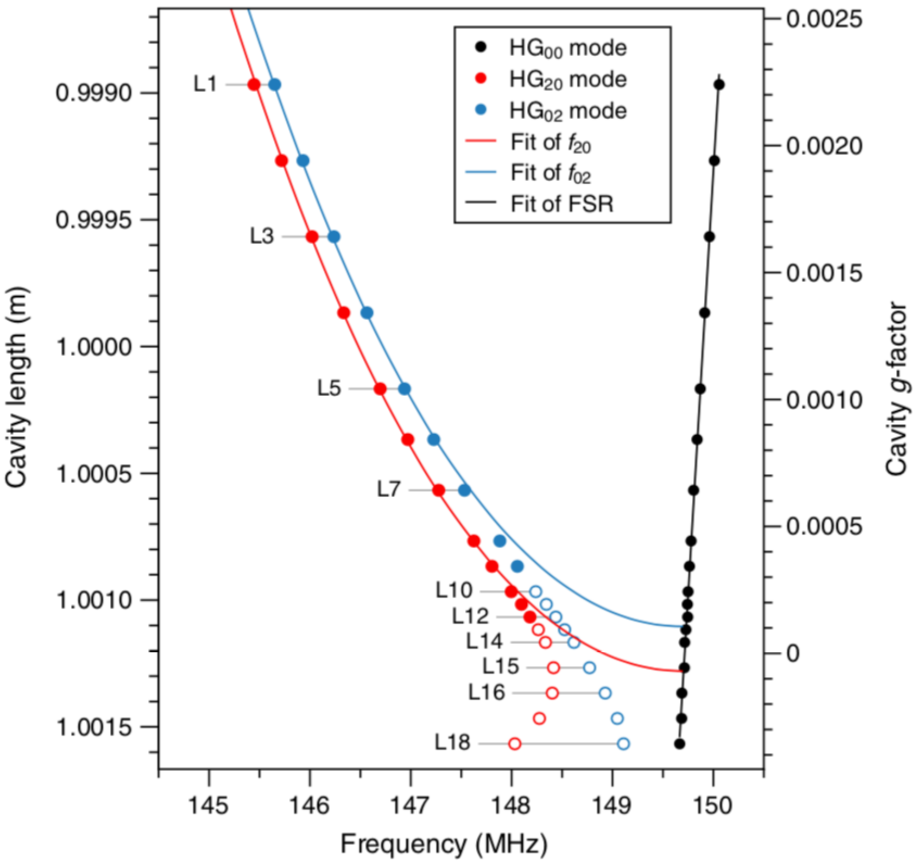

$$L_0 + \Delta L = \frac{R_{2+}}{2}\left[1 - \cos\left(\frac{f_{20}}{\mathrm{FSR}}\pi\right)\right]$$

$$L_0 + \Delta L = \frac{R_{2-}}{2}\left[1 - \cos\left(\frac{f_{02}}{\mathrm{FSR}}\pi\right)\right]$$

R_{2+} = 1,001,284.9 ± 4.6 μm

R_{2-} = 1,001,140.0 ± 15.7 μm

Fitting the map with Zernike polynomials

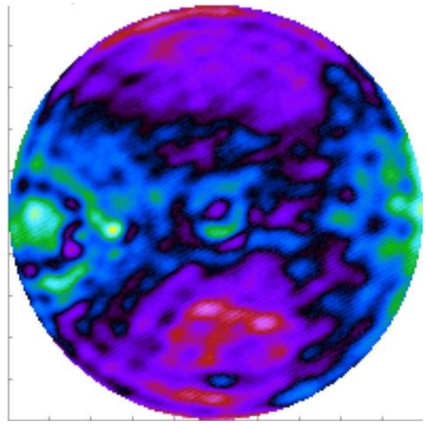

Original map

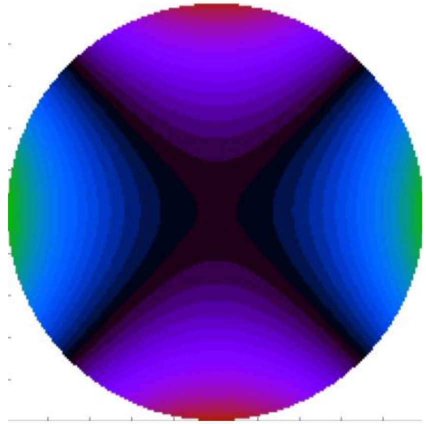

Zernike map order 2

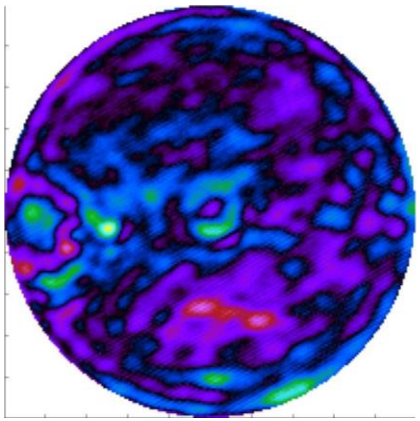

Residue

Astigmatism

R_{2+} = 1,001,300.7 μm 15.8 μm

R_{2-} = 1,001,133.2 μm -6.8 μm

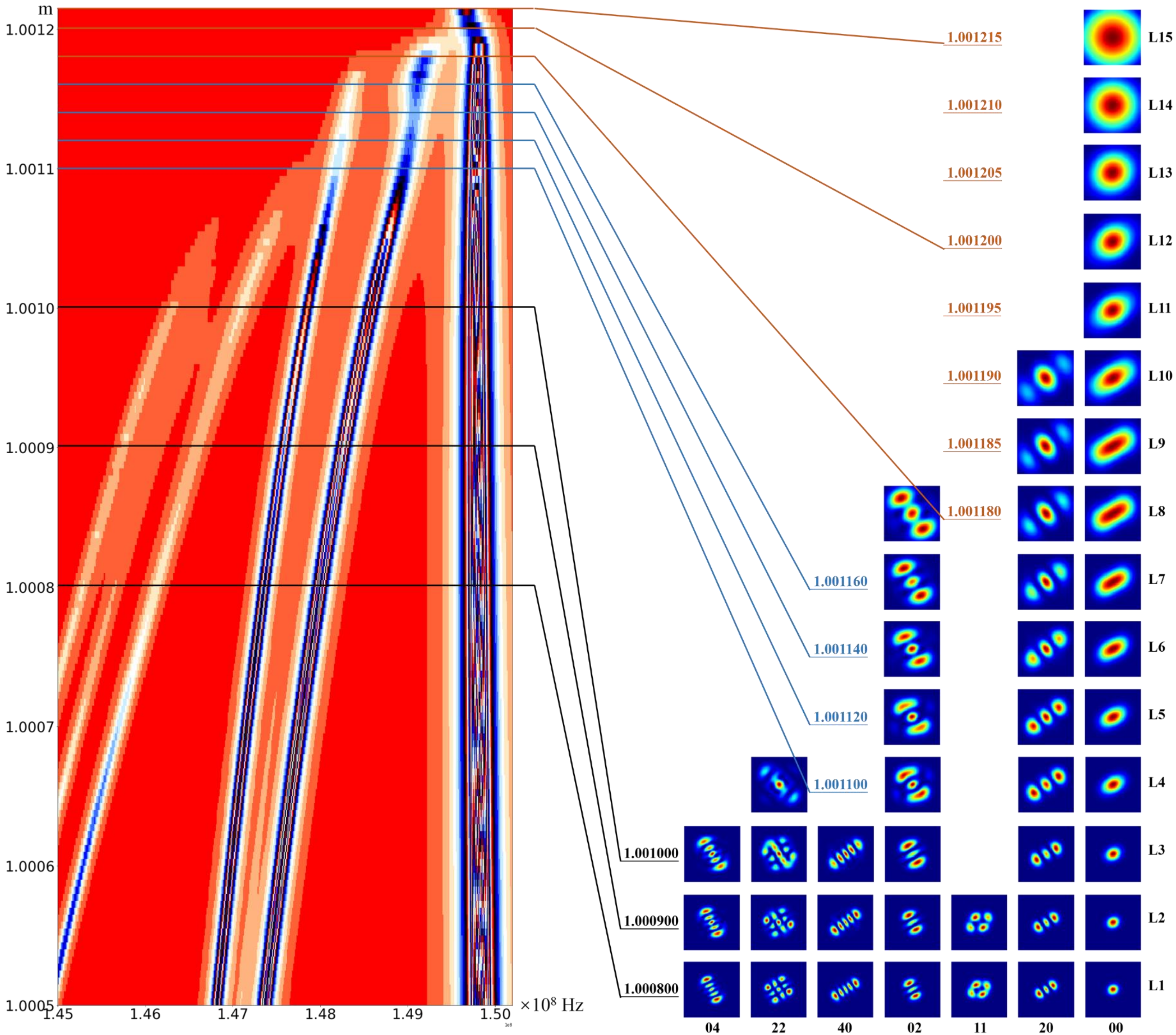
m
1.0012
1.0011
1.0010
1.0009
1.0008
1.0007
1.0006
1.0005
1.45
1.46
1.47
1.48
1.49
1.50
×10^8 Hz
1.001215
1.001210
1.001205
1.001200
1.001195
1.001190
1.001185
1.001180
1.001160
1.001140
1.001120
1.001100
1.001000
1.000900
1.000800
L15
L14
L13
L12
L11
L10
L9
L8
L7
L6
L5
L4
L3
L2
L1
04
22
40
02
11
20
00

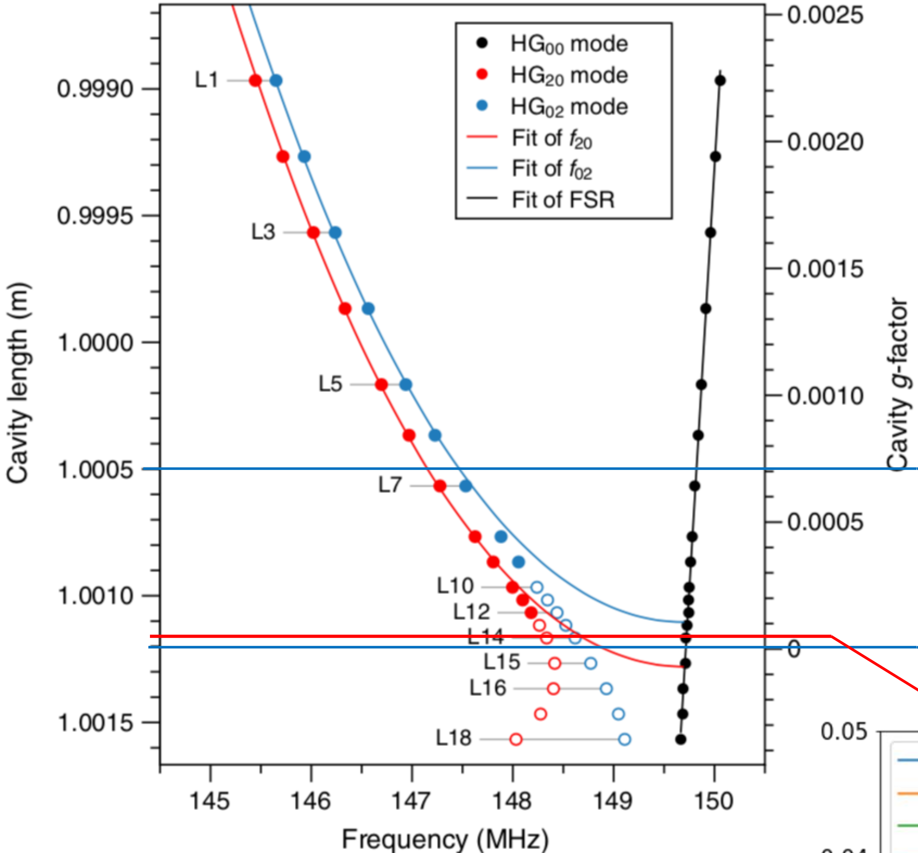

The maximum HOM order taken into account for calculation is 6.

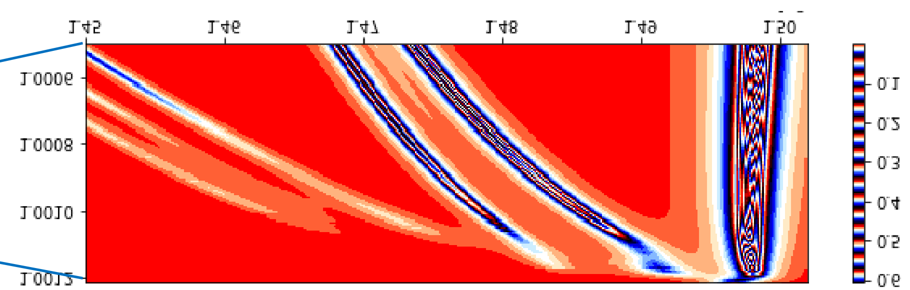

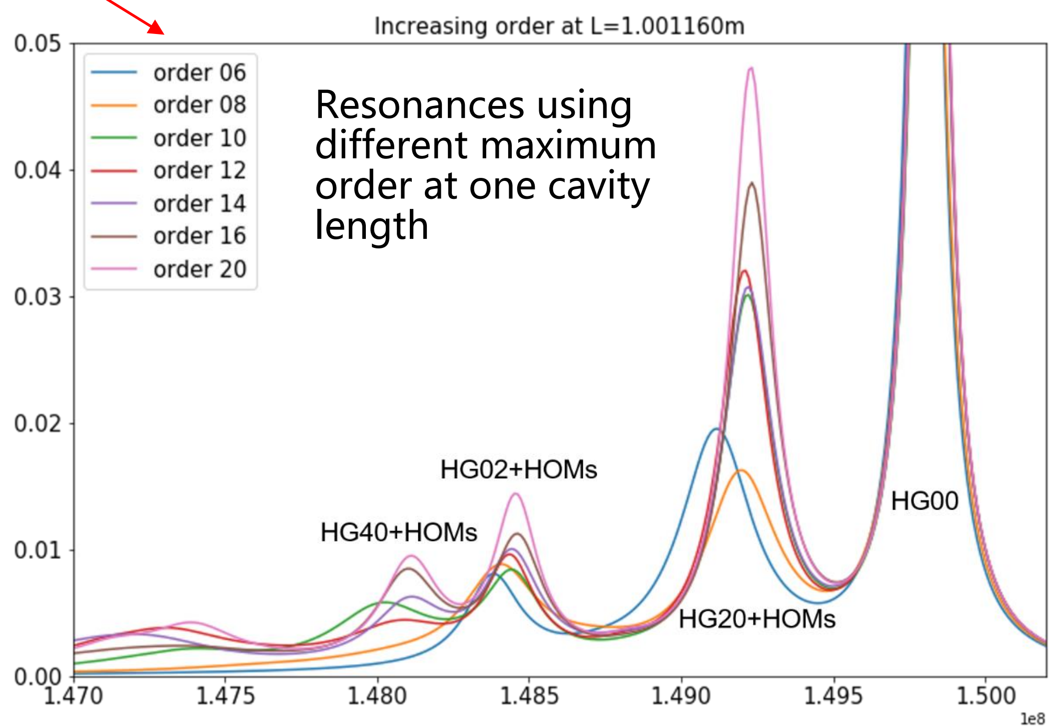

Resonances using different maximum order at one cavity length

However, the maximum order of HOMs for calculation does matter very much.

The higher the maximum order taken into account, the longer the calculation time.

4. Study of birefringence effect in KAGRA

- Backgrounds
  - ➢ Birefringence is a severe problem in KAGRA.
  - ➢ Around 5%~10% s-pol light is coupled to p-pol due to birefringence of the sapphire mirror.

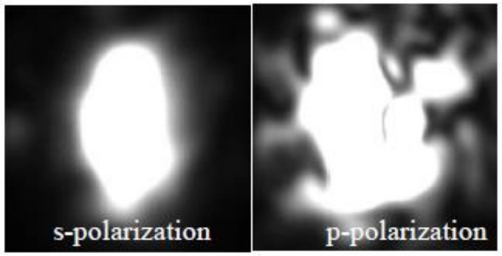

- Purpose of this study
  - ➢ To understand the influence of the birefringence by comparing numerical simulations with experimental measurements.
  - ➢ To find ways of mitigating the birefringence effect so that the interferometer can achieve its design sensitivity.

4. Study of birefringence effect in KAGRA

- Model: a two-world approach

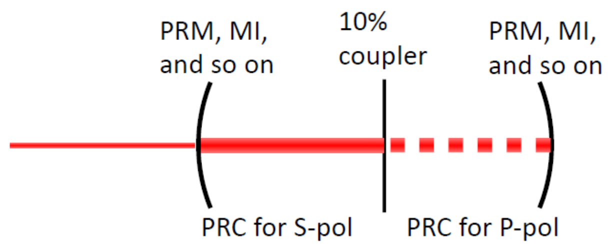

S-pol and p-pol beams form a coupled cavity.

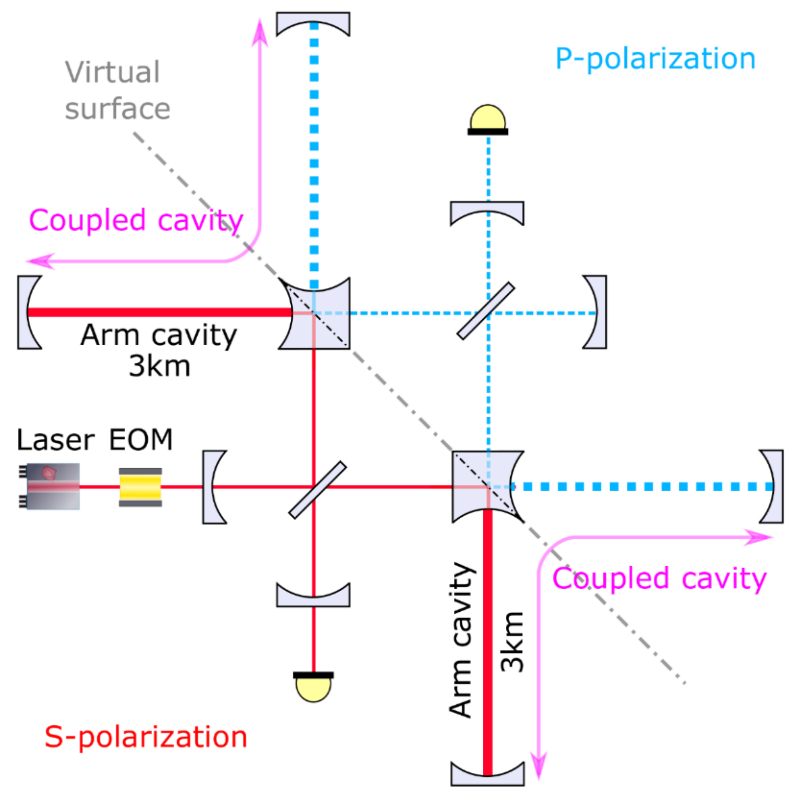

We have

- figured out the phase relation in s/p couplings
- derived the coupling matrix
- proposed a model to simulate birefringence with Finesse

We are going to

- derive the birefringence map
- set up the two-world approach model in Finesse
- apply necessary mirror maps to study birefringence

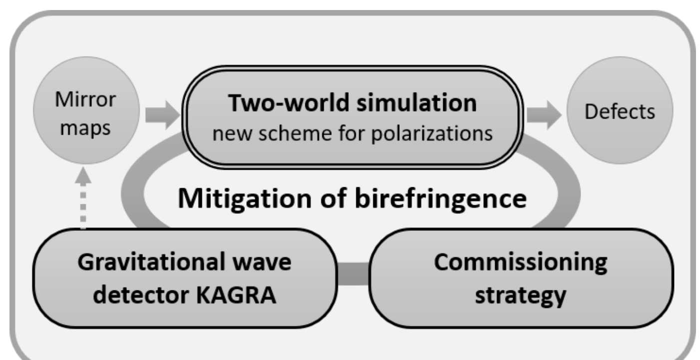

4. Study of birefringence effect in KAGRA

Coupling matrix

JGW-T2012048

JGW-T1910380

Thickness: *d*

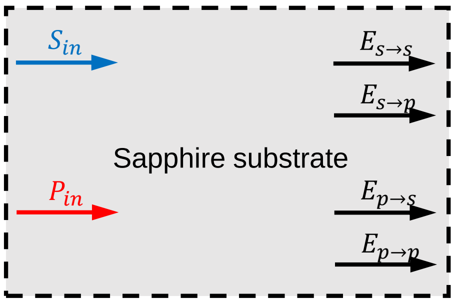

$$\alpha_e = 2\pi\frac{dn_e'}{\lambda} \qquad \alpha_o = 2\pi\frac{dn_o}{\lambda}$$

Note $\alpha_e = \alpha_+ + \alpha_-$
$\alpha_o = \alpha_+ - \alpha_-$

One-way phase difference α_-

$$\alpha_- = \frac{\alpha_e - \alpha_o}{2} = \frac{\pi d}{\lambda}(n_e' - n_o)$$

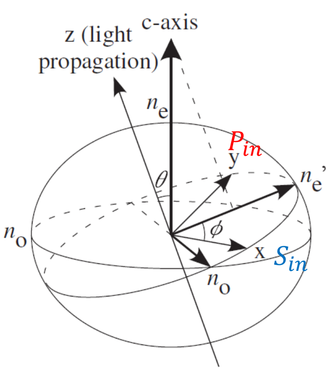

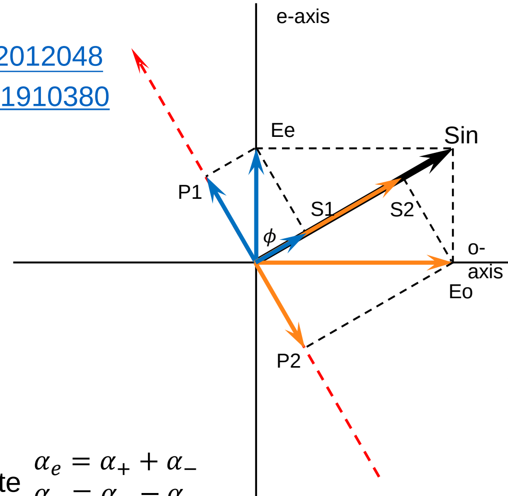

Considering the incident beam is pure s-pol Sin. It is projected to e-axis and o-axis. After a propagation of thickness d, the two fields are

$$E_e = \cos\phi\, e^{i\alpha_e}S_{in} \qquad E_o = \sin\phi\, e^{i\alpha_o}S_{in}$$

The two fields are then projected back to s-pol axis and p-pol axis:

$$\begin{aligned}E_{s\to s} &= \cos\phi E_e + \sin\phi E_o = S_{in}\left(\cos^2\phi e^{i\alpha_e} + \sin^2\phi e^{i\alpha_o}\right)\\ &= S_{in}e^{i\alpha_+}\left(\cos^2\phi e^{i\alpha_-} + \sin^2\phi e^{-i\alpha_-}\right)\\ &= S_{in}e^{i\alpha_+}[\cos^2\phi(\cos\alpha_- + i\sin\alpha_-) + \sin^2\phi(\cos\alpha_- - i\sin\alpha_-)]\\ &= S_{in}e^{i\alpha_+}(\cos\alpha_- + i\cos 2\phi\sin\alpha_-)\end{aligned}$$

$$\begin{aligned}E_{s\to p} &= \sin\phi E_e - \cos\phi\, E_o = S_{in}\left(\sin\phi\cos\phi\, e^{i\alpha_e} - \sin\phi\cos\phi\, e^{i\alpha_o}\right)\\ &= S_{in}e^{i\alpha_+}\left(\sin\phi\cos\phi\, e^{i\alpha_-} - \sin\phi\cos\phi\, e^{-i\alpha_-}\right)\\ &= S_{in}e^{i\alpha_+}\cdot i\sin 2\phi\sin\alpha_-\end{aligned}$$

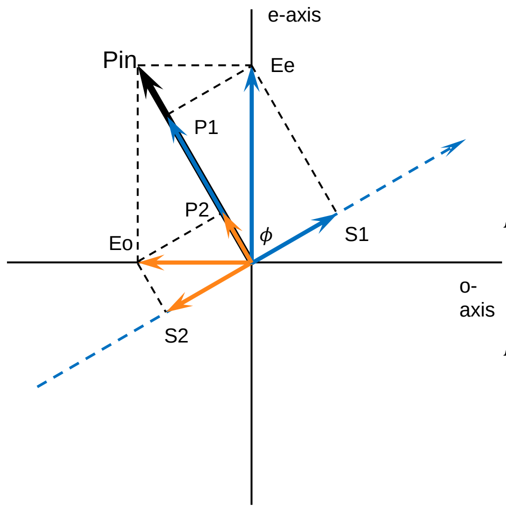

Considering the incident beam is pure p-pol Pin. It is projected to e-axis and o-axis. After a propagation of thickness d, the two fields are

$$E_e = \sin\phi\, e^{i\alpha_e}P_{in} \qquad E_o = \cos\phi\, e^{i\alpha_o}P_{in}$$

The two fields are then projected back to s-pol axis and p-pol axis:

$$\begin{aligned}E_{p\to s} &= \cos\phi E_e - \sin\phi\, E_o = P_{in}\left(\sin\phi\cos\phi\, e^{i\alpha_e} - \sin\phi\cos\phi\, e^{i\alpha_o}\right)\\ &= P_{in}e^{i\alpha_+}\left(\sin\phi\cos\phi\, e^{i\alpha_-} - \sin\phi\cos\phi\, e^{-i\alpha_-}\right)\\ &= P_{in}e^{i\alpha_+}\cdot i\sin 2\phi\sin\alpha_-\end{aligned}$$

$$\begin{aligned}E_{p\to p} &= \sin\phi\, E_e + \cos\phi\, E_o = P_{in}\left(\sin^2\phi e^{i\alpha_e} + \cos^2\phi e^{i\alpha_o}\right)\\ &= Pe^{i\alpha_+}\left(\sin^2\phi e^{i\alpha_-} + \cos^2\phi e^{-i\alpha_-}\right)\\ &= P_{in}e^{i\alpha_+}[\sin^2\phi(\cos\alpha_- + i\sin\alpha_-) + \cos^2\phi(\cos\alpha_- - i\sin\alpha_-)]\\ &= P_{in}e^{i\alpha_+}(\cos\alpha_- - i\cos 2\phi\sin\alpha_-)\end{aligned}$$

4. Study of birefringence effect in KAGRA

We have developed a model to simulate the birefringence.

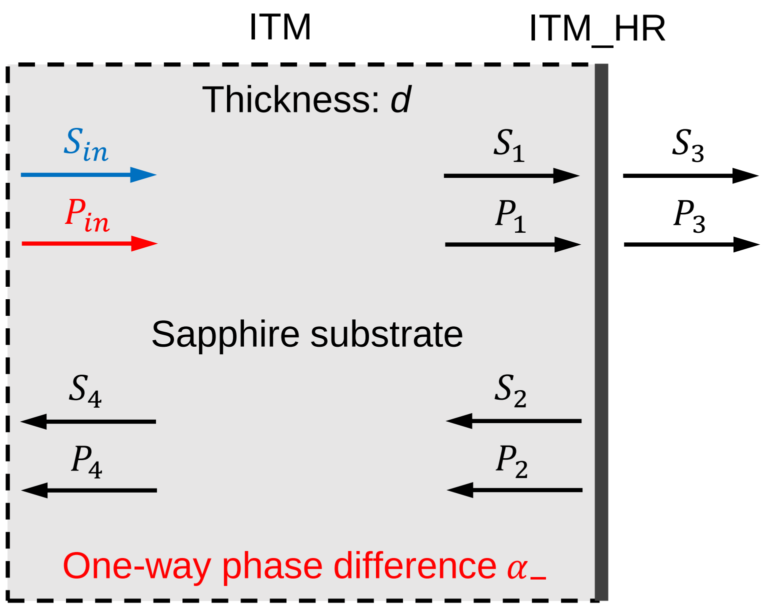

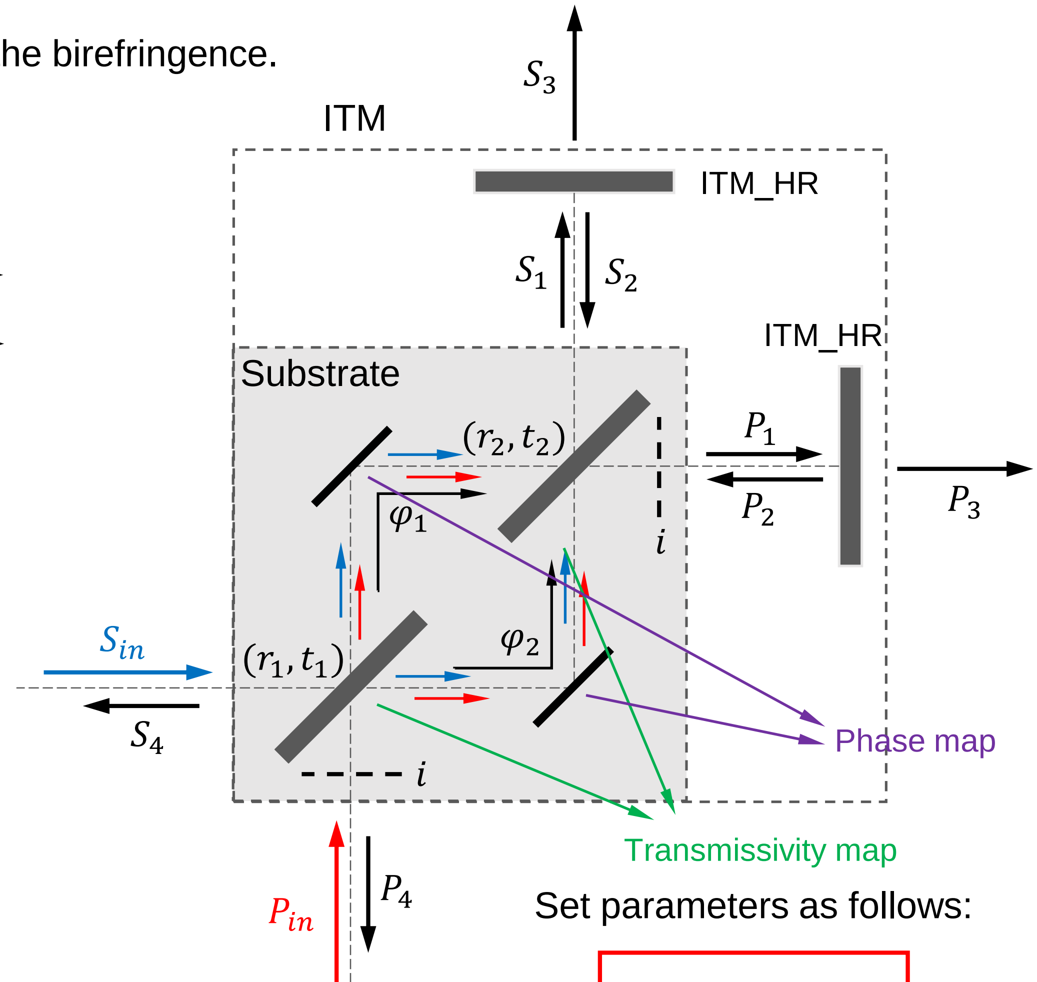

$$\alpha_- = \frac{\alpha_e - \alpha_o}{2} = \frac{\pi d}{\lambda}(n_e' - n_o)$$

In both cases, we have fields as follows

$$\begin{bmatrix} S_1 \\ P_1 \end{bmatrix} = \boldsymbol{G} \times \begin{bmatrix} S_{in} \\ P_{in} \end{bmatrix} \quad \begin{bmatrix} S_2 \\ P_2 \end{bmatrix} = r_{HR} \begin{bmatrix} S_1 \\ P_1 \end{bmatrix} \quad \begin{bmatrix} S_3 \\ P_3 \end{bmatrix} = i t_{HR} \begin{bmatrix} S_1 \\ P_1 \end{bmatrix} \quad \begin{bmatrix} S_4 \\ P_4 \end{bmatrix} = \boldsymbol{G} \times \begin{bmatrix} S_2 \\ P_2 \end{bmatrix}$$

$$\boldsymbol{G} = \begin{bmatrix} r_{s\to s} & t_{p\to s} \\ t_{s\to p} & r_{p\to p} \end{bmatrix} = \begin{bmatrix} \cos\alpha_- + i\cos 2\phi \sin\alpha_- & i\sin 2\phi \sin\alpha_- \\ i\sin 2\phi \sin\alpha_- & \cos\alpha_- - i\cos 2\phi \sin\alpha_- \end{bmatrix}$$

Set parameters as follows:

$$r_1 = r_2 = \sin\phi$$
$$t_1 = t_2 = \cos\phi$$
$$\varphi_1 = -\alpha_-$$
$$\varphi_2 = \pi + \alpha_-$$

4. Study of birefringence effect in KAGRA

Measure the transmission wavefront error (TWE) map

Fig. 1

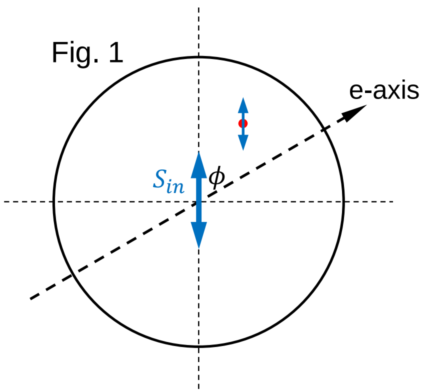

Fig. 2

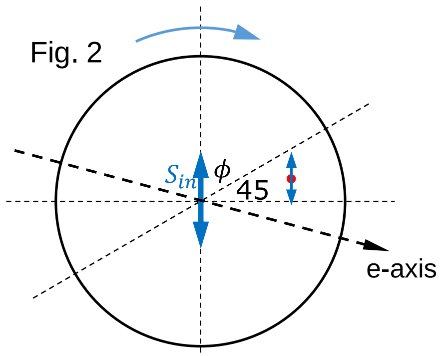

Clockwise rotate the mirror by 45 degrees and measure the map

Fig. 3

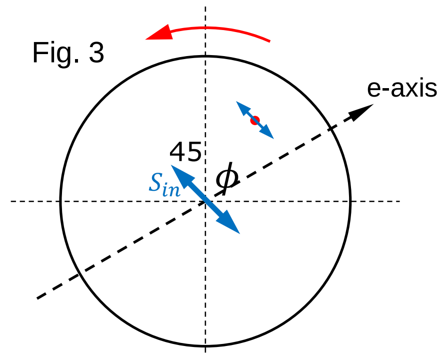

The measured map is anticlockwise rotated back by 45 degrees.

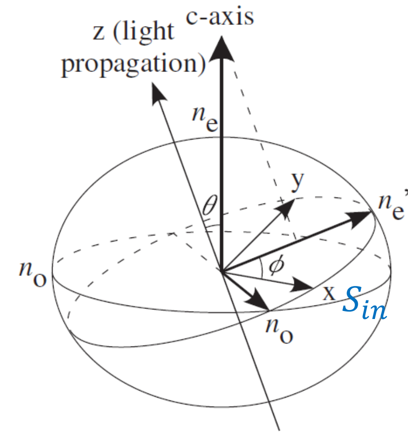

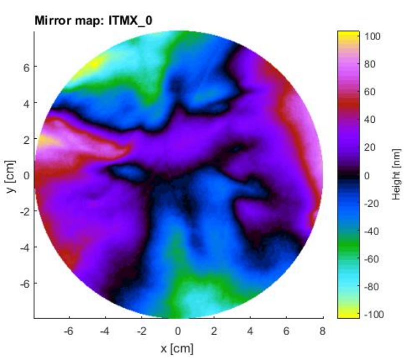

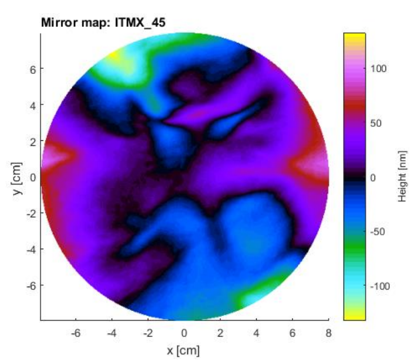

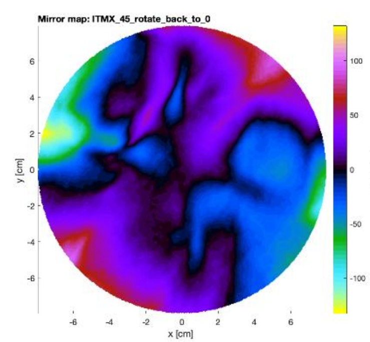

After rotating the map back, it is equivalent that we change the polarization rotation of the input beam and take the measurement, while the mirror keeps still. (Compare Fig. 1 and Fig. 3.)

4. Study of birefringence effect in KAGRA

TWE maps for ITMX

$map(0)$

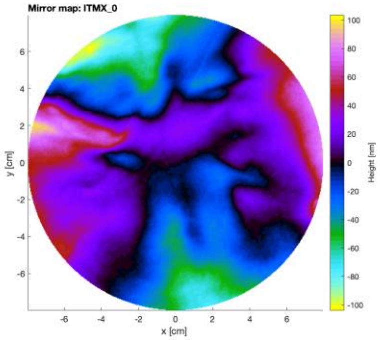

$map(45)$

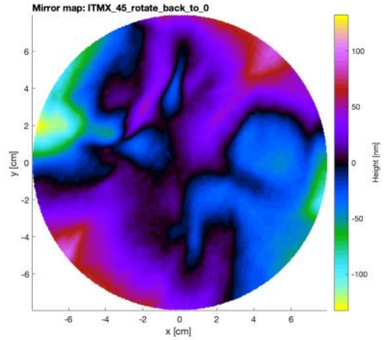

$map(90)$

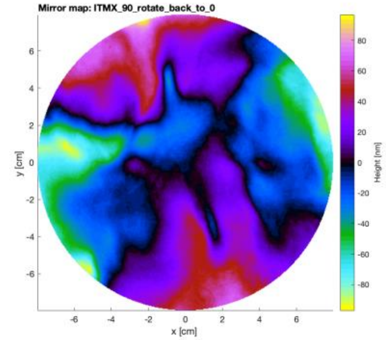

$map(135)$

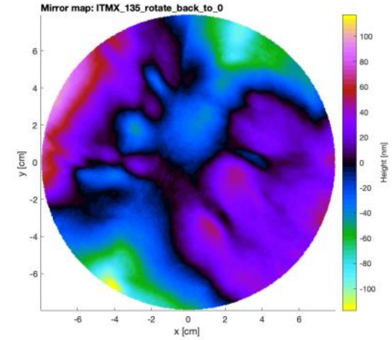

$map(180)$

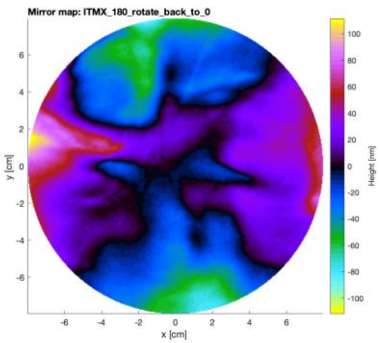

$map(225)$

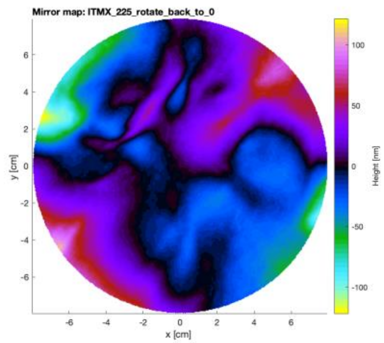

$map(270)$

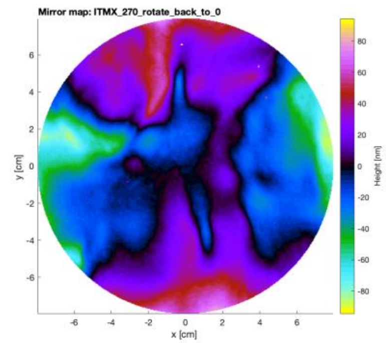

$map(315)$

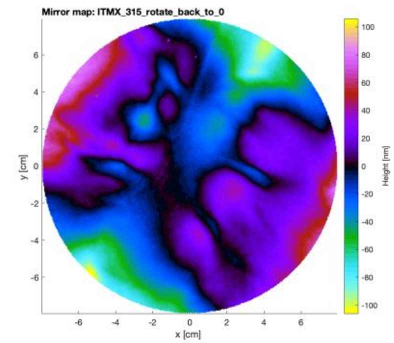

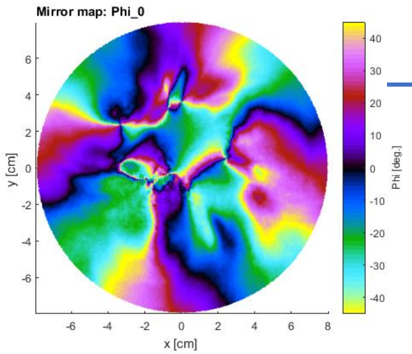

$$\phi = -\frac{1}{2}\tan^{-1}\frac{map(\phi+45) - map(\phi+135)}{map(\phi) - map(\phi+90)}$$

$$\alpha_{-} = \frac{\alpha_e - \alpha_o}{2} = \frac{2\pi}{\lambda}\cdot\frac{map(\phi) - map(\phi+90)}{\cos 2\phi}$$

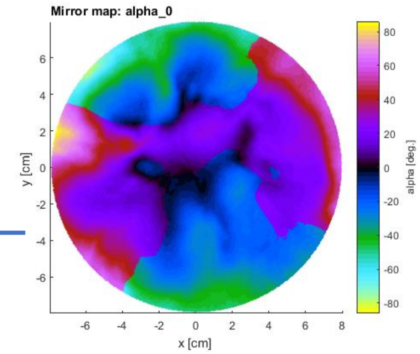

4. Study of birefringence effect in KAGRA

- Check resonances for p-pol beam
- Check control signals
- Check power recycle gain
- Check beam shapes
- Perform modal mode analysis
- ....

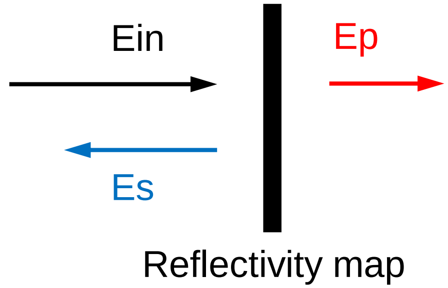

Single bounce beam shape

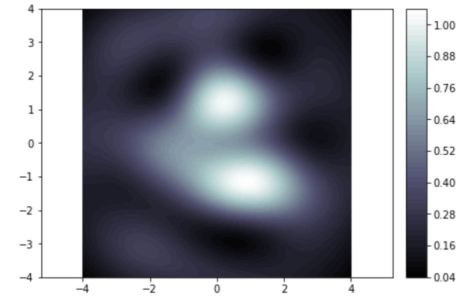

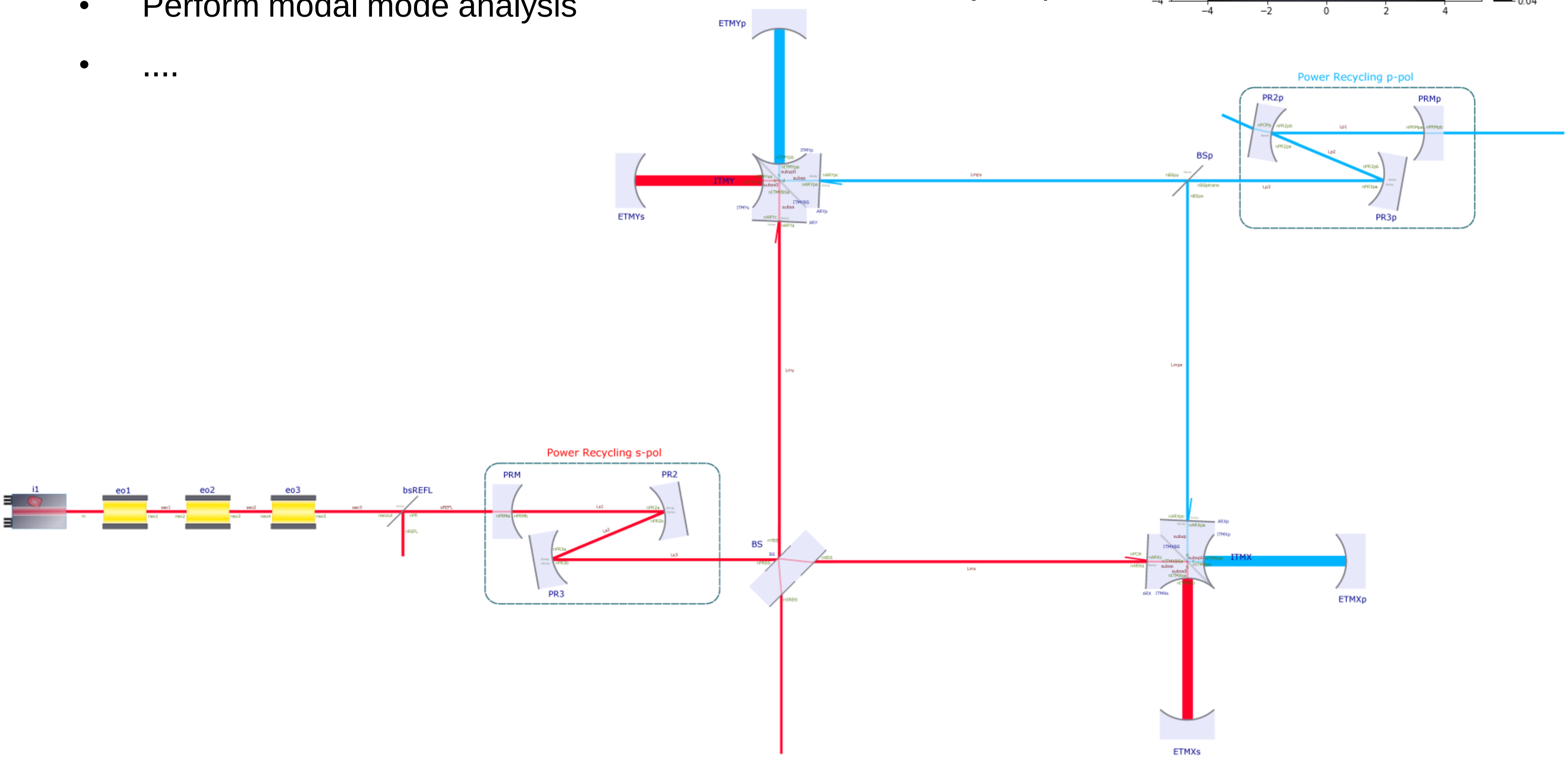

Thank you !